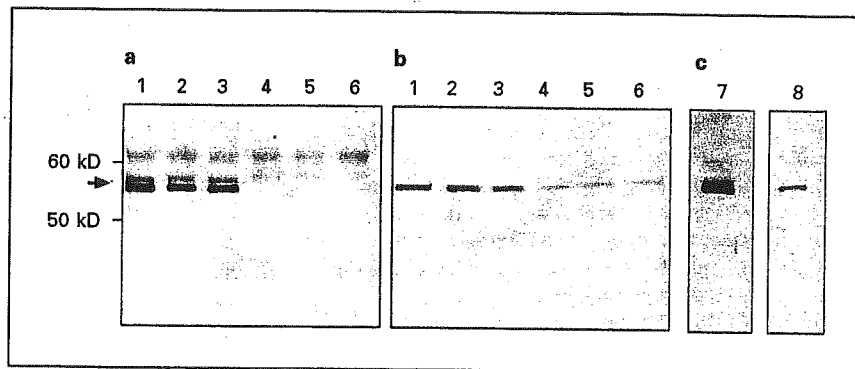


**Fig. 1.** Myocilin RNA expression in transfected COS-1 cells. 1: Negative control (no transfection); 2: wild type; 3: R158Q; 4: D208E; 5: I360N; 6: A363T; 7: I477S.



**Fig. 2.** Western blot analysis of intracellular and secreted myocilin from wild-type and mutant transfected into COS-1 cells. Intracellular (a) and secreted (b) myocilin was detected by anti-human myocilin peptide antibody. c Specificity of the antibody was tested by absorption test using antigen peptide. Details described in Materials and Methods. Lane 1: wild type; 2: R158Q; 3: D208E; 4: I360N; 5: A363T; 6: I477S; 7: secreted wild type; 8: secreted wild-type + antigen peptide.

**Table 1.** Number of study subjects with sequence alterations detected in the *MYOC* gene

Sequence alteration	NTG patients (n = 80)	Control subjects (n = 100)	p values <sup>1</sup>
R-46-Stop (136 C to T)	2 (2.5)	0 (0)	0.20
R-76-K (227 G to A)	7 (8.8)	3 (3)	0.11
R-158-Q (473 G to A)	2 (2.5)	0 (0)	0.20
D208-E (624 C to G)	3 (3.8)	5 (5)	0.50
A 488-A (1464 C to T)	1 (1.3)	0 (0)	0.45
3'non-coding (1515 + 73 G to C)	3 (3.8)	1 (0)	0.24

Figures in parentheses are percentages.

<sup>1</sup> Fisher's exact probability test.

Co-transfection of COS-1 cells with wild type and one mutant *MYOC* (I360N) led to the suppression of intracellular and extracellular secretion of myocilin (fig. 3).

The antibody used for this experiment was tested for specificity by an antigen peptide absorbance test (fig. 2c). The antigen peptide significantly reduced the myocilin signal in Western blotting, demonstrating the specificity of the antibody. The secondary antibody alone did not show any signals.

### Discussion

Myocilin is expressed in the trabecular meshwork, ciliary body, retina, and the optic nerve head [14, 19, 20]. In recent studies, intracellular as well as extracellular expression of myocilin has been reported in astrocytes and lamina cribrosa cells of the optic nerve head [14, 21]. These observations suggest the possible involvement of myocilin in the glaucomatous damage of the optic nerve head.

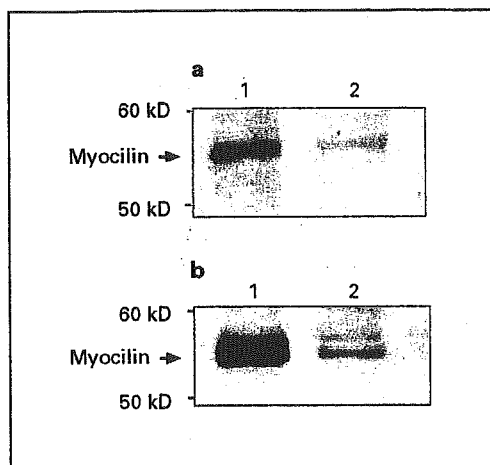


**Fig. 3.** Western blot analysis of intracellular and secreted myocilin from wild type and mutant co-transfected into COS-1 cells. Wild-type myocilin and equal amount of variant I360N were mixed and transfected into COS-1 cells. The intracellular (a) and secreted (b) myocilin was detected by anti-human myocilin peptide antibody. 1: wild type, 2: co-transfection (wild type: I360N = 1:1).

Thus, the question arose whether mutations in the *MYOC* gene were also associated with NTG. The Q368stop [12] and T293K [22] variant have been reported in patients with NTG. On the other hand, Clark et al. [14] suggested that coding sequence variations in myocilin were not commonly involved in the NTG phenotype. However, they reported three polymorphisms, L215P, T256M, and W286R, in 3 of the 307 NTG patients, while none was detected in 193 controls [14]. These variants may possibly be associated with the NTG phenotype.

We have identified 6 variants of *MYOC*, one of which did not cause an amino acid substitution (A488A), and another existed in a non-coding region. R76K is considered to be a non-disease-causing polymorphism worldwide [7, 8, 23]. The R46Stop variant was identified in two Japanese NTG patients, and in none of the normal Japanese controls. In the Chinese population, subjects with a heterozygous R46Stop had POAG or were normal, and those with a homozygous R46Stop did not have glaucoma [18]. This mutation was also detected in 4 of 132 normal Chinese controls. In the Korean population, a patient with a homozygous R46Stop had severe juvenile-onset POAG [24], and this mutation was also detected in 1 of 106 normal Korean controls. Thus, the clinical phenotype of R46Stop is not consistent with the genotype, and the reduction in the amount of myocilin expression associat-

ed with this mutation may not necessarily cause glaucoma.

Variant R158Q was found in 2 Japanese NTG patients but not in the 100 control subjects in the present study. However, Mabuchi et al. [13] have previously reported this variant in 1 of 100 Japanese controls. Variant D208E was also found in Japanese control subjects. A group in the United States reported this variant as a possible disease-causing variant for glaucoma [23]. A statistically significant p value for these three sequence variations, R46Stop, R158Q, and D208E, was not obtained between NTG patients and controls. However, to clarify the prevalence of *MYOC* mutations in association with NTG, a large number of NTG patients and controls will be needed for a statistical study.

Jacobson et al. [16] demonstrated that myocilin was expressed in the cell and was secreted into the medium of ocular (trabecular meshwork) or non-ocular cells (COS-1) transformed with wild-type *MYOC* or a polymorphic variant (K398R), but one variant (G364V) showed limited secretion and others (Q368X, K423GE, Y437H, I477S) showed none. Myocilin was secreted from cultured cells but very little or no myocilin was secreted from cells expressing mutant forms of *MYOC* that are located in the olfactomedin-like domain and associated with POAG.

We have designed a simple functional test using the readily available COS-1 cell line to monitor myocilin secretion by the variant forms of *MYOC* found in patients with POAG or NTG. In the present study, five missense variants were examined for secretory function. Of the 5 *MYOC* variants, R158Q and D208E located in the myocilin-like domain were identified in patients with NTG; I360N and A363T located in the olfactomedin-like domain were identified in our previous study in Japanese patients with POAG [9], and the L477S variant was reported by Jacobson et al. [16] in a patient with juvenile-onset POAG [17]. L477S was used as pathological control for protein secretion.

In this functional test, the I360N, A363T, and L477S variants were non-secreting, while the R158Q and D208E variants secreted myocilin. The expression and secretion level of myocilin in variants R158Q and D208E were similar to those of the wild type myocilin. No myocilin accumulation was observed in cells transfected with non-secreting variants. When wild-type *MYOC* was co-transfected with mutant I360N, a significant reduction of wild type myocilin was observed in these cells. These observations led us to suggest that the mutant protein is not only degraded quickly in the cells but also influences the stability of the wild-type myocilin. A dominant-negative mech-

anism may have been the causative effect in I360N myocilin. Whether this is caused by dimerization of the wild type and mutant is under investigation.

It is well established that mutations in the olfactomedin-like domain of myocilin result in altered secretion [16]. Variants R158Q and D208E are not located in the olfactomedin-like domain, and R158Q is located in the myocin-like domain. However, it has not been established whether mutations in the myocin-like domain of myocilin result in altered secretion in vitro. Thus, impaired secretion is not the only mechanism involved in NTG, and there is a possibility that alterations in myocilin contrib-

ute to NTG along with other factors. Further investigations are needed to clarify the association of *MYOC* with NTG.

### Acknowledgements

This research was supported by Research on Eye and Ear Sciences from Ministry of Health, Labor and Welfare of Japan. This research was also supported by Scientific Research (B) and Exploratory Research from the Ministry of Education, Science, Sports and Culture of Japan. The authors thank Dr. Duco Hamasaki for editorial comments.

### References

- Ishida K, Yamamoto T, Sugiyama K, et al: Disk hemorrhage is a significantly negative prognostic factor in normal-tension glaucoma. *Am J Ophthalmol* 2000;129:707-714.
- Kamal D, Hitchings R: Normal tension glaucoma - a practical approach. *Br J Ophthalmol* 1998;82:835-840.
- Drance S, Anderson DR, Schulzer M: Risk factor for progression of visual field abnormalities in normal-tension glaucoma. *Am J Ophthalmol* 2001;131:699-708.
- Stone EM, Fingert JH, Sheffield VC, et al: Identification of a gene that causes primary open angle glaucoma. *Science* 1997;275:668-670.
- Kubota R, Noda S, Wang Y, et al: A novel myosin-like protein (myocilin) expressed in the connecting cilium of the photoreceptor: Molecular cloning, tissue expression, and chromosomal mapping. *Genomics* 1997;41:360-369.
- Shimizu S, Lichter PR, Johnson AT, et al: Age-dependent prevalence of mutations at the *GLC1A* locus in primary open-angle glaucoma. *Am J Ophthalmol* 2000;130:165-177.
- Alward WLM, Fingert JH, Coote MA, et al: Clinical features associated with mutations in the chromosome 1 open-angle glaucoma gene (*GLC1A*). *N Engl J Med* 1998;338:1022-1027.
- Fingert JH, Heon E, Liebmann JM, et al: Analysis of myocilin mutations in 1,703 glaucoma patients from five different populations. *Hum Mol Genet* 1999;8:899-905.
- Kubota R, Mashima Y, Ohtake Y, et al: Novel mutations in the myocilin gene in Japanese glaucoma patients. *Hum Mutat* 2000;16:270. Online Citation: Human Mutation, Mutation in Brief #355.
- Lam DS, Leung YF, Chua JK, et al: Truncations in the *TIGR* gene in individuals with and without primary open-angle glaucoma. *Invest Ophthalmol Vis Sci* 2000;41:1386-1391.
- Kubota R, Kudoh J, Mashima Y, et al: Genomic organization of the human myocilin gene (*MYOC*) responsible for primary open angle glaucoma (*GLC1A*). *Biochem Biophys Res Commun* 1998;242:396-400.
- Mardin CY, Velton I, Ozbey S, et al: A *GLC1A* gene Gln368Stop mutation in a patient with normal-tension open-angle glaucoma. *J Glaucoma* 1999;8:154-156.
- Mabuchi F, Yamagata Z, Kashiwagi K, et al: Analysis of myocilin gene mutations in Japanese patients with normal tension glaucoma and primary open-angle glaucoma. *Clin Genet* 2001;59:263-268.
- Clark AF, Kawase K, Stone EM, et al: Expression of the glaucoma gene myocilin (*MYOC*) in the human optic nerve head. *FASEB J* 2001;15:1251-1253.
- Shiose Y, Kitazawa Y, Tsukahara S, et al: Epidemiology of glaucoma in Japan - a nationwide glaucoma survey. *Jpn J Ophthalmol* 1991;35:133-135.
- Jacobson N, Andrews M, Sheffield VC, et al: Non-secretion of mutant proteins of the glaucoma gene myocilin in cultured trabecular meshwork cells and in aqueous humor. *Hum Mol Genet* 2001;10:117-125.
- Adam MF, Belmouden A, Binisti P, et al: Recurrent mutations in a single exon encoding the evolutionarily conserved olfactomedin-homology domain of *TIGR* in familial open-angle glaucoma. *Hum Mol Genet* 1997;6:2091-2097.
- Lam DSC, Leung YF, Chua JKH, et al: Truncation in the *TIGR* gene in individuals with and without primary open-angle glaucoma. *Invest Ophthalmol Vis Sci* 2000;41:1386-1391.
- Huang W, Jaroszecki J, Caca-Prados M, et al: Expression of the *TIGR* gene in the iris, ciliary body, and trabecular meshwork of the human eye. *Ophthalmic Genet* 2000;21:155-169.
- Swiderski RE, Ross JL, Fingert JH, et al: Localization of *MYOC* transcripts in human eye and optic nerve by in situ hybridization. *Invest Ophthalmol Vis Sci* 2000;41:3420-3428.
- Noda S, Mashima Y, Obazawa M, et al: Myocilin expression in the astrocytes of the optic nerve head. *Biochem Biophys Res Commun* 2000;276:1129-1135.
- Williams-Lyn D, Flanagan J, Buys Y, et al: The genetic aspects of adult-onset glaucoma: A perspective from the Greater Toronto area. *Can J Ophthalmol* 2000;35:12-17.
- Alward WLK, Kwon YH, Khanna CL, et al: Variations in the myocilin gene in patients with open-angle glaucoma. *Arch Ophthalmol* 2002;120:1189-1197.
- Yoon SJK, Kim HS, Moon JI, et al: Mutations of the *TIGR/MYOC* gene in primary open-angle glaucoma in Korea. *Am J Hum Genet* 1999;64:1775-1778.

# Purification, Molecular Cloning, and Expression of a Novel Growth-Promoting Factor for Retinal Pigment Epithelial Cells, REF-1/TFPI-2

Yasubiko Tanaka,<sup>1</sup> Jun Utsumi,<sup>2</sup> Mizuo Matsui,<sup>3</sup> Tetsuo Sudo,<sup>2</sup> Noriko Nakamura,<sup>2</sup> Masato Mutoh,<sup>2</sup> Akemi Kajita,<sup>2</sup> Saburo Sone,<sup>2</sup> Kazuteru Kigasawa,<sup>4</sup> Masabiko Shibuya,<sup>1</sup> Venkat N. Reddy,<sup>5</sup> Qiang Zhang,<sup>1,6</sup> and Takeshi Iwata<sup>1</sup>

**PURPOSE.** Retinal pigment epithelial (RPE) cells are known to play important roles in maintaining the homeostasis of the retina and in controlling choroidal neovascularization. The purpose of this study was to identify a factor or factors that would stimulate RPE cells to proliferate.

**METHODS.** To isolate such a factor, 100 L of human-fibroblast-conditioned medium underwent ion-exchange, hydrophobic, and reverse-phase chromatographies followed by sodium dodecyl sulfate-polyacrylamide gel electrophoresis. The growth-promoting activity of the factor was examined in a human K-1034 RPE cell line and human primary RPE cells.

**RESULTS.** The different chromatographic processes isolated a 31-kDa factor that had RPE cell growth-promoting properties. This factor, which we have named RPE cell factor (REF)-1, promotes growth of RPE cells but not of human umbilical vein endothelial cells (HUVECs). The amino-terminal sequence and molecular cloned cDNA of REF-1 were identical with those of tissue-factor pathway inhibitor (TFPI)-2, a family of TFPIs, and placental protein (PP)-5, a serine protease inhibitor. The cDNA expression of REF-1/TFPI-2 with pcDL-pSR $\alpha$  vector in Chinese hamster ovary (CHO) cells confirmed the growth-promoting activity for RPE cells. The major component of the recombinant REF-1/TFPI-2 expressed in CHO cells had a molecular mass of 31 kDa and exerted growth-promoting activity in RPE cells but not in human endothelial cells and fibroblasts in vitro. REF-1/TFPI-2 also had protease inhibitory activity. The other family factor, TFPI-1, did not promote RPE cell growth.

**CONCLUSIONS.** REF-1/TFPI-2 is a novel growth-promoting factor for RPE cells but not for endothelial cells and fibroblasts. Its properties make it potentially beneficial for intraocular therapy for the repair and maintenance of RPE cells. (*Invest Ophthalmol Vis Sci.* 2004;45:245-252) DOI:10.1167/iov.03-0230

Recent advances in basic and clinical research have shown that the pathogenesis of many retinal and choroidal diseases is closely related to the normal functioning of retinal pigment epithelial (RPE) cells. RPE cells play critical roles in maintaining the homeostasis of the retina and in controlling choroidal neovascularization.<sup>1</sup> Because the denaturation of cellular proteins in the RPE and the loss of function of RPE cells are responsible for retinal and choroidal diseases, a factor that stimulates RPE cell growth could prove to be valuable for the treatment of RPE-related ocular diseases.

At present, various cell growth factors, such as basic fibroblast growth factor (bFGF) and platelet-derived growth factor (PDGF), are known to stimulate the proliferation of RPE cells.<sup>2-4</sup> However, these factors are also known to affect the growth of vascular endothelial cells and fibroblasts,<sup>5-7</sup> and ocular neovascularization and fibroblast proliferation can lead to serious retinal and choroidal diseases and proliferative vitreoretinopathy.

The purpose of this study was to isolate and characterize a factor or factors that would promote RPE cell proliferation. We focused on the supernatant of cultured human fibroblasts as a source of the target factor, because fibroblasts function as stromal cells that are known to produce various cytokines. We have isolated a 31-kDa factor from the conditioned medium of human fibroblasts that promotes growth in RPE cells and named it RPE cell factor (REF)-1. The amino terminal sequence was determined, and molecular cloning of its cDNA showed that the factor was identical with tissue-factor pathway inhibitor (TFPI)-2<sup>8</sup>-placental protein 5 (PP5).<sup>9</sup>

## MATERIALS AND METHODS

### Isolation of RPE Cell Growth-Promoting Factor

Human fibroblast DIP-2 cells<sup>10</sup> were cultured for 5 days in Eagle's minimum essential medium (MEM) supplemented with 5% fetal calf serum (FCS) in microcarriers (Cytodex I; Amersham Biosciences, Tokyo, Japan) in 16-L glass culture vessels at 37°C. After the addition of 100 IU/mL human interferon- $\beta$  (Toray Industries, Tokyo, Japan) as a priming agent and 10  $\mu$ g/mL poly(D) poly(C) (Yamasa Shouyu, Choushi, Japan) as a cytokine-inducing reagent, the culture media was replaced by serum-free Eagle's MEM and cultured at 37°C for six additional days.

The cultured medium was collected and filtered to remove the cellular debris. Fractionation was started by passing 100 L of the cultured medium through an S-Sepharose column (500 mL; Amersham Biosciences), and the fraction containing growth-promoting activity (active fraction) was eluted with 200 mL of 10 mM phosphate-buffered

From the <sup>1</sup>National Institute of Sensory Organs, National Tokyo Medical Center, Tokyo, Japan; the <sup>2</sup>Pharmaceutical Research Laboratories, Toray Industries, Inc., Kamakura, Japan; the <sup>3</sup>Department of Ophthalmology, Nihon University Surugadai Hospital, Tokyo, Japan; the <sup>4</sup>Department of Ophthalmology, Tokai University School of Medicine, Isehara, Japan; the <sup>5</sup>Department of Ophthalmology, Kellogg Eye Center, University of Michigan, Ann Arbor, Michigan; and the <sup>6</sup>Department of Ophthalmology, Keio University School of Medicine, Tokyo, Japan.

Supported in part by grants for Research on Sensory and Communicative Disorders by the Ministry of Health, Labor and Welfare, Japan and by National Eye Institute Grants EY00484 and EY07003.

Submitted for publication March 5, 2003; revised September 1, 2003; accepted September 4, 2003.

Disclosure: Y. Tanaka, None; J. Utsumi, Toray Industries (F, E, P); M. Matsui, None; T. Sudo, Toray Industries (F, E); N. Nakamura, Toray Industries (F, E); M. Mutoh, Toray Industries (F, C, P); A. Kajita, Toray Industries (F, E); S. Sone, Toray Industries (F, E); K. Kigasawa, None; M. Shibuya, None; V.N. Reddy, None; Q. Zhang, None; T. Iwata, None

The publication costs of this article were defrayed in part by page charge payment. This article must therefore be marked "advertisement" in accordance with 18 U.S.C. §1734 solely to indicate this fact.

Corresponding author: Yasuhiko Tanaka, National Institute of Sensory Organs, National Tokyo Medical Center, 2-5-1 Higashigaoka, Meguro-ku, Tokyo 152-8902, Japan; ytanaka@ntmc.hosp.go.jp.

saline (PBS) at pH 7.4 with 0.5 M NaCl. The eluate was added to 1 M ammonium sulfate and applied to a polypropyl A column (0.8 × 25 cm; PolyLC, Columbia, MD). The active protein was eluted by a gradient of 0 to 1 M ammonium sulfate in 10 mM PBS. Four milliliters of the active fraction from the polypropyl A column were injected into a C4 reverse-phase column (1 × 25 cm; Grace Vydac, Hesperia, CA), and the protein was eluted by a gradient of water-acetonitrile (0%-70%) including 0.1% trifluoroacetic acid (TFA; pH 2.0). Two milliliters of the active fraction eluted from the column was concentrated to 100  $\mu$ L by speed vacuum concentrator (Speed Vac Systems, Savant, MN) and applied to sodium dodecyl sulfate-polyacrylamide gel electrophoresis (SDS-PAGE) under nonreducing conditions without 2-mercaptoethanol (2ME). Immediately after migration of the sample into the gel, the SDS-PAGE gel was cut into 1 × 2 × 4-mm slices and immersed overnight at 4°C in 0.5 mL per slice of distilled water to extract the active protein. The extracted protein was reappplied to SDS-PAGE under reducing-nonreducing conditions to examine the purity and the molecular weight of the target protein.

### Determination of Cell Growth-Promoting Activity during Purification

Human K-1034 RPE cells or fourth-passage human primary RPE cells were used to determine RPE cell growth-promoting activity.<sup>11</sup> K-1034 cells or human primary RPE cells were added to collagen type I-coated 24-well plastic plates (Corning International, Tokyo, Japan) at a density of  $1 \times 10^4$  cells/well. DMEM supplemented with 5% FCS (Invitrogen Japan, Tokyo, Japan) or 15% FCS (Invitrogen) was used for K-1034 or human primary RPE cells, respectively. Two microliters of purified REF-1 was added to each well and cultured at 37°C for 5 days. The number of RPE cells at each time point was determined by a cell counter (model ZM; Beckman Coulter K. K., Tokyo, Japan). The growth-promoting rate was calculated as a percentage of the control ( $n = 4$  or 6). In the first exploratory purification, the specific concentration of REF-1 was not determined, as an REF-1 ELISA kit is not available, and REF-1 was therefore traced by the growth-promoting activity in RPE cells.

### Determination of Cell Growth-Promoting Activity Using Purified REF-1 Protein

To examine whether purified REF-1 promotes growth in the number of vascular endothelial cells, cells were isolated from the human umbilical vein of a patient at an obstetric hospital. In accordance with the provisions of the Declaration of Helsinki, all subjects signed an informed consent after an explanation of the procedures to be used and the purpose of the studies. The human umbilical vein endothelial cells (HUVECs) were treated under conditions similar to those used for RPE cells ( $n = 4$  or 6). Human fibroblasts (DIP-2 cells), rabbit primary RPE cells, and human primary RPE cells were also used to characterize the growth-promoting activity ( $n = 6$ ).

A comparison of the growth-promoting profile of other related factors, such as TFPI-1 (American Diagnostica, Greenwich, CT), the family of TFPIs, ciliary neurotrophic factor (CNTF; R&D Systems, Minneapolis, MN), and bFGF (R&D Systems), was performed at a concentration of 10 ng/mL ( $n = 6$ ).

### Amino Acid Analyses of REF-1/TFPI-2

REF-1 was isolated as a  $31 \pm 3$ -kDa protein on SDS-PAGE gel under nonreducing conditions. The active fraction appeared to correspond to a single band on the silver-stained gel. REF-1 was isolated from the band and subjected to amino-terminal amino acid sequence analysis (Protein sequencer model 470; Applied Biosystems Japan, Tokyo, Japan).

Amino acid composition analysis of REF-1 component was performed after hydrolysis at 110°C for 22 and 72 hours in 6 M HCl with 4% thioglycolic acid (amino acid analyzer model 835; Hitachi, Tokyo, Japan).

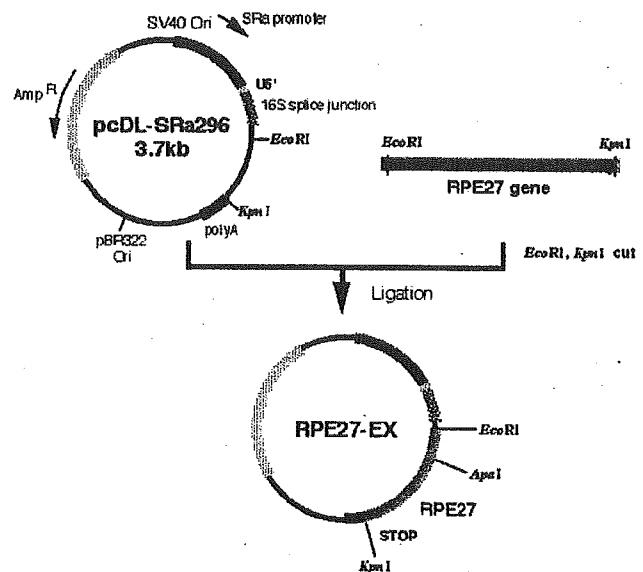


FIGURE 1. The construction of the REF-1 expression vector. The RPE27-EX1 expression vector was obtained by ligation with pcDL-SRa296 vector (3.7 kb) and RPE27 gene (750 bp).

### Molecular Cloning of REF-1 Protein

The primers, R1: 5'-GGAAGAAGGCACATGGC-3', R2: 5'-TATGGGGAT-TGGTGGCG-3', R3: 5'-ACTCCTGGAGCCCGTC-3', L1: 5'-AGACATG-GCCTGCCCG-3', L2: 5'-GACACCAGACCAACTGG-3', and L3: 5'-GG-TAGCGACCGGCGC-3' were used for PCR amplification of phage insert and were designed based on the sequence of cloning vector  $\lambda$ gt11 (Human placenta cDNA library, CLHL1008b; BD Biosciences-Clontech Japan, Tokyo, Japan). The first PCR was performed with primers, R1 and L1, designed to flank the insert of  $\lambda$ gt11. The second PCR was performed using 1  $\mu$ L of the first PCR reaction mixture as template with three primers: 27S1 (5'-GATGCIGAACAAGAACCIACIG-3') and the R2 and L2 primers. The third PCR was performed with the second PCR mixture as a template, with primer 27S2 (5'-CAAGAACCIACIG-GIACIAATGC-3') and the R3 and L3 primers.

The PCR conditions were initiated at 94°C for 5 minutes, then 25 cycles at 94°C for 30 seconds, 56°C for 2 minutes, and 72°C for 8 minutes, followed by 1 cycle at 72°C for 7 minutes. The amplified DNA fragment from the third PCR was separated by 1% agarose gel electrophoresis and the DNA fragment was purified from gel by the electroelution method. Purified DNA fragment was cloned using a kit (Sure Clone; Amersham Bioscience). The nucleotide sequence was determined for 16 clones containing full-length cDNA on a DNA sequencer (model 373A; Applied Biosystems).

### Construction of Expression Vector for REF-1/TFPI-2

REF-1 cDNA was reamplified by PCR from an original  $\lambda$ gt11 phage clone by primer set RPE27-EX1 (5'-GGGGAATTCCTTCTCGGACG-GCTTGC-3') and RPE27-EX2 (5'-GGGGGTACCTAAAAATTGCTTCTT CCG-3') to obtain the insert for the expression vector. PCR was performed for 25 cycles in a reaction mixture with 0.2  $\mu$ g of  $\lambda$ gt11 DNA, 1.6 mM dNTP, 1.0  $\mu$ M of primers (RPE 27-EX1 and RPE 27-EX2), and DNA polymerase (Ex Taq; Takara, Tokyo, Japan). The PCR product was digested with *Eco*RI and *Kpn*I and ligated into expression vector pcDL-SRa296 to obtain expression vector RPE27-EX (Fig. 1).<sup>12</sup>

### Expression of Recombinant REF-1/TFPI-2 by CHO Cells

The expression vector RPE27-EX and the expression vector pAddHFR containing dihydrofolate reductase (DHFR) cDNA were cotransfected

into the DHFR gene-deficient CHO DXB11 cell strain. The surviving DHFR-positive cells were selected in  $\alpha$ MEM without ribonucleosides and deoxyribonucleosides with 10% FCS. Highly producible cells were then selected by addition of methotrexate (MTX) to the medium. The concentration was increased stepwise from 0.0025  $\mu$ M, to 0.05  $\mu$ M, and finally to 1  $\mu$ M, to obtain highly producible cells.<sup>12</sup>

After reaching confluence, the culture medium was replaced by serum-free  $\alpha$ MEM and the medium was collected every 2 days, nine times. The collected medium was centrifuged at 6000 rpm at 4°C for 15 minutes, filtered, and stored at 4°C until the large-scale purification procedures.

### Preparation of Anti-REF-1/TFPI-2 Antibody and ELISA

Peptide antibody for REF-1/TFPI-2 was generated, using peptide NH<sub>2</sub>-SGGCHRNRIENRFPDE-COOH, corresponding to residues 106-120 as an antigen. Rabbit antiserum was purified on a protein A column (Prosep A; Amersham Biosciences). A sandwich ELISA system was constructed by using primary antibody (5  $\mu$ g/mL) generated against whole REF-1 protein, biotinylated secondary peptide antibody (5.2  $\mu$ g/mL) raised against amino acids 106 through 120, and the avidin HRP anti-rabbit antibody. During the process of REF-1 purification, protein quantification was determined by this ELISA kit with detection sensitivity of 10 ng/mL.

### Purification of CHO Cell-Derived Recombinant REF-1/TFPI-2

Forty liters of culture supernatant was applied to a gel filtration column (S-Sepharose FF, 5  $\times$  15 cm, 300 mL; Amersham Biosciences) at 2.4 L/h and the column was washed with 1.2 L of 20 mM sodium citrate buffer (pH 5.0) and 1.7 L of buffer containing 0.2 M NaCl. Protein was eluted by 20 mM sodium citrate (pH 5.0)/0.4 M NaCl. TFA was added to the eluate at a final concentration of 0.1% and further purified by reverse-phase chromatography (Resource RPC column, 0.46  $\times$  10 cm, 3 mL; Amersham Biosciences). The elution was performed with acetonitrile gradient of 0% to 70% in 0.1% TFA (pH 2.0). REF-1 was eluted in 19 mL of 31% to 35% acetonitrile fraction. This fraction was diluted with 40 mM PBS (pH 7.2) to twofold volume and applied to a gel filtration

column (SP-Sepharose FF, 1  $\times$  1.3 cm, 1 mL; Amersham Biosciences). REF-1 was eluted with 20 mM PBS (pH 7.2) containing 0.45 M NaCl.

### Determination of Protease Inhibitor Activity

Plasmin inhibition by REF-1 was analyzed by a method introduced previously.<sup>13</sup> Reaction buffer (50 mM Tris-HCl [pH 7.5], 5 mM CaCl<sub>2</sub>, 0.1 M NaCl, 0.01% Tween 20) was added to 96-well plastic plates followed by the addition of 0.4  $\mu$ g aprotinin (Boehringer-Yamanouchi, Tokyo, Japan) and REF-1/TFPI-2 at final concentration of 5  $\mu$ g/mL. One hundred twenty-five nanograms of plasmin was added (Chromogenix, Milano, Italy) and incubated at room temperature for 30 minutes. Fifty microliters of substrate S-2251 (Val-Leu-Lys-pNA, 1 mg/mL; Chromogenix) was added and the absorbance was measured at 405 to 450 nm for 15 minutes with a microplate photometer (UV/Visible Spectrometer DU640; Beckman Coulter, Fullerton, CA) every 20 seconds. The percentage of relative activity in the inhibitor concentration was then calculated.

### Determination of RPE Cell Production of Cytokines

The relationship between RPE cell growth and production of the growth factor bFGF, transforming growth factor (TGF)- $\beta$ 1, transforming growth factor (TGF)- $\beta$ 2, epidermal growth factor (EGF), granulocyte colony-stimulating factor (G-CSF), granulocyte-macrophage CSF (GM-CSF), and macrophage-CSF (M-CSF), and the cytokines interleukin (IL)-1 $\alpha$ , IL-6, IL-8, tumor necrosis factor (TNF)- $\alpha$  by human primary RPE cells was examined. The cells were grown in DMEM with 15% FCS for 3 days and the medium then replaced by serum-free DMEM. The cytokines in the culture supernatant were determined for two additional days by ELISA kits (Amersham International, Buckinghamshire, UK; R&D Systems, Minneapolis, MN; Immuno-Biological Laboratories, Gunma, Japan).

### Western Blot Analysis of REF-1 for RPE Cell Extract

Cellular extract was obtained from RPE cells by using M-PER (Pierce, Rockford, IL) detergent mixture. A sample amount of 7.2  $\mu$ g was

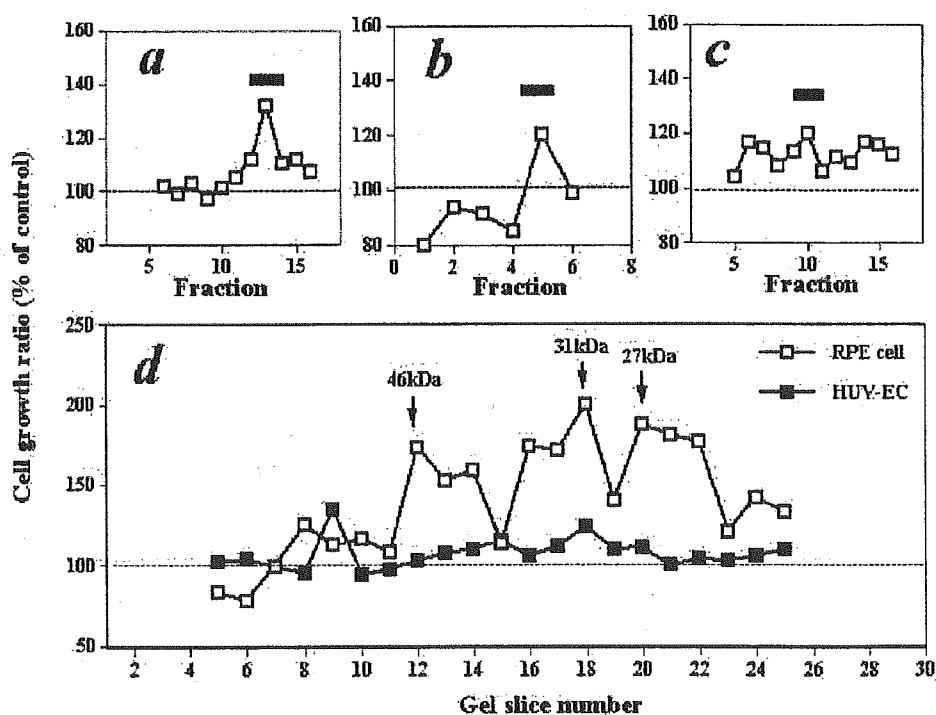
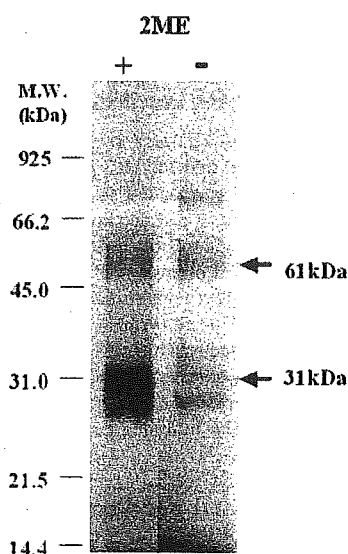


FIGURE 2. Chromatography was used to determine RPE cell growth-promoting activity. Profiles of the activity on S-Sepharose (a), polypropyl-A (b), and Vydac-C4 (c) columns and on a nonreducing SDS-PAGE gel (d). Data denote active fractions collected. In the SDS-PAGE fraction, the growth-promoting activity was examined in RPE cells and HUVECs.



**FIGURE 3.** SDS-PAGE pattern of the RPE cell growth-promoting factor REF-1 isolated from the conditioned medium of human fibroblasts. Approximately 1  $\mu\text{g}/\text{lane}$  of the purified protein was loaded and made visible with silver staining after electrophoresis under reducing (+2ME) and nonreducing (-2ME) conditions. A major band at 31 kDa and a minor band at 61 kDa correspond to the monomeric and dimeric forms of REF-1, respectively.

applied to each lane in 12% polyacrylamide gels. For positive control, bacteria expressing REF-1 protein was added (see Fig. 7, lane 4). After the separation, proteins were transferred to a nitrocellulose membrane (Schleicher & Schuell, Relliehausen, Germany), blocked for 1 hour with the blocking solution containing 10% milk diluent-blocking solution (KPL, Gaithersburg, MD) and 0.1% Tween-20 in phosphate-buffered saline (pH 7.4). The membrane was probed with a rabbit polyclonal anti-REF-1 antibody (1  $\mu\text{g}/\text{mL}$ ). The specific signal was detected by incubation of anti-rabbit IgG HRP secondary antibody (New England BioLabs, Beverly, MA) followed by chemiluminescence reactions with luminol reagent A and peroxide reagent B, as recommended by the manufacturer (New England BioLabs) and made visible with a chemiluminescence imager (Lumi-Imager F1; Roche Applied Science, Tokyo, Japan).

#### RNA Isolation from RPE cells and RT-PCR of REF-1

Total RNA was isolated from cultured fourth-passage human primary RPE cells with a total RNA isolation kit (RNA-Bee-RNA Isolation Reagent; Tel-Test, Friendswood, TX). Total RNA samples were digested by RNase-free DNase (Roche Diagnostics Japan) to minimize the risk of genomic DNA contamination. First-strand cDNA was synthesized using random primers (SuperScript First-Strand Synthesis System for RT-PCR; Invitrogen Japan). PCR was performed using 1  $\mu\text{g}$  of single-strand cDNA with 2.5U *Taq* DNA polymerase in a volume of 50  $\mu\text{L}$ . After predenaturation at 95°C for 5 minutes, 30 cycles were performed, including denaturation at 95°C for 30 seconds, annealing at 65°C for 30

seconds, and extension at 72°C for 1 minute, followed by 1% agarose gel electrophoresis. The primers used were: 5'-ATTCTGCTGCTTTTC-CTGAC-3' (sense primer) and 5'-CAGCTCTGCGTGTACCTGTC-3' (antisense primer).

## RESULTS

### Isolation and Identification of an RPE Cell Growth-Promoting Factor

The RPE cell growth-promoting fraction was purified from 100 L of starting material to 0.5 mL of SDS-PAGE gel extract. REF-1 was concentrated by  $2 \times 10^5$ -fold after the final step of purification. The profile of the RPE cell growth-promoting factor is shown at each step in Figure 2. The peak of RPE cell growth promotion was mainly detected in three fractions of molecular mass  $46 \pm 3$ ,  $31 \pm 3$ , and  $27 \pm 3$  kDa on the SDS-PAGE gel. The 31-kDa fraction had the highest RPE cell growth-promoting effect. This fraction showed very low growth stimulation in HUVECs for all molecular sizes detected. The 31-kDa active fraction was separated from the SDS-PAGE gel under reducing-nonreducing conditions. The 31-kDa band was made visible as a major component by silver staining (Fig. 3). There was a minor component at 61 kDa that was predicted as a dimeric form of REF-1. Amino-terminal sequence analysis was performed on the purified 31-kDa protein.

### Amino-Terminal Sequence of RPE Cell Growth-Promoting Factor

Amino-terminal sequence analysis of the 31-kDa component resulted in the following sequence:  $\text{NH}_2\text{-Asp-Ala-Glu-Gln-Pro-Thr-Gly-Thr-Asn-Ala-Glu-Ile-Xaa-Ala-COOH}$  (14 amino acids).

In addition, amino-terminal sequence analysis of the 27-kDa component gave nine residues of sequences identical with the 31-kDa component. The polypeptide was named REF-1. Because the amino-terminal sequence of REF-1 was apparently identical with TFPI-2<sup>8</sup>-PP5,<sup>9</sup> molecular cloning of REF-1 was performed to confirm the whole sequence of the 31-kDa protein. For the 46-kDa active component isolated on SDS-PAGE gel, the amino acid sequence could not be identified because of insufficient quantity of the protein.

### Molecular Cloning of REF-1

Although REF-1 was identical with TFPI-2 at the amino-terminal, molecular cloning was performed to determine the complete cDNA of REF-1. One of the 16 clones isolated had an amino-terminal sequence identical with that of TFPI-2. The cloned REF-1 molecule consisted of 235 amino acids, and the theoretical molecular mass of this polypeptide was 27 kDa. The position of three tandemly arranged Kunitz-type domains and two binding sites of predicted asparagine-linked sugar chains were identical with TFPI-2. From the available evidence, we concluded that REF-1 is identical with TFPI-2. The calculated molecular mass increased by 4 to 6 kDa after possible glycosylation to molecular mass between 31 and 33 kDa.

**TABLE 1.** Purification of CHO-Cell-Derived Recombinant REF-1

Purification Step	Volume (mL)	Protein Conc ( $\mu\text{g}/\text{mL}$ )	Total Protein (mg)	REF-1 (mg)	Yield (%)	Purity (%)	Purification (x)
CHO cell CM	40,000.0	113.8	4552.0	10.8	100	0.24	1
S-Sepharose	800.0	82.8	66.2	8.6	80	13.00	54
Resource RPC	40.0	159.0	6.4	6.4	59	87.00	360
SP-Sepharose	4.2	913.0	3.8	3.8	35	97.00	400

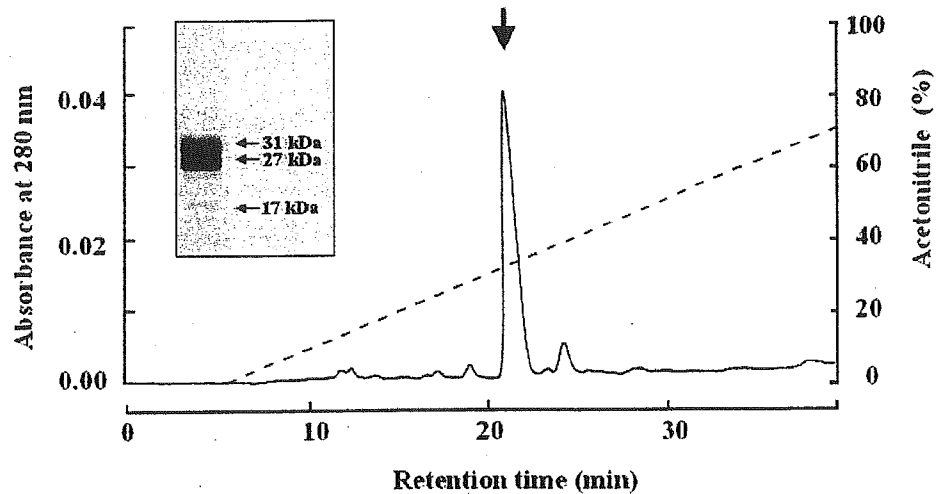


FIGURE 4. Reverse-phase chromatographic profile of CHO-cell-derived recombinant REF-1 in a final purification step. SDS-PAGE was used to amplify recombinant REF-1. Approximately 5  $\mu$ g of the purified protein was loaded and made visible with Coomassie blue R-250 staining after electrophoresis under reducing (+2ME) conditions. Major components at 31 and 27 kDa and a minor component at 17 kDa were observed.

### Purification of CHO Cell-Derived Recombinant REF-1

We developed a large-scale purification procedure for CHO cell-derived recombinant REF-1. From 40 L of conditioned medium of recombinant REF-1-CHO cells, recombinant REF-1 was purified by the combination of cation exchange chromatography and reverse-phase high-performance liquid chromatography (HPLC) as shown in Table 1. The purity of the final recombinant REF-1 was more than 97% on SDS-PAGE gel and was free of pyrogen. The reverse-phase HPLC profile and SDS-PAGE pattern of purified CHO cell-derived recombinant REF-1 are shown in Figure 4.

### Molecular Heterogeneity of REF-1

A molecular heterogeneity of the CHO-cell-derived recombinant REF-1 was observed. Three forms of REF-1 at molecular masses of  $31 \pm 1$ ,  $27 \pm 1$ , and  $17 \pm 1$  kDa were found. The ratios for each size were approximately 40% for 31 kDa, 50% for 27 kDa, and 10% for 17 kDa. The 31- and 27-kDa components were major and appeared to be different because of attached sugar chains. The 17-kDa component was smaller than the theoretical molecular mass by approximately 10 kDa. This form was possibly produced by extracellular protease digestion after the secretion of the mature form based on the amino acid composition analysis. The molecular mass of 10

kDa was calculated to match the 28-kDa component lacking the C-terminal portion.

Currently, data are not available for the differences in biological effects of the different molecular forms. TFPI-2 also demonstrated molecular heterogeneity of 31 and 27 kDa, and it has been suggested that this may be due to different glycosylated forms.<sup>14</sup>

### Cell Growth-Promoting Activity of Recombinant REF-1

The growth-promoting activity of REF-1 in K-1034 cells was dose dependent, with a bell-shaped curve (Fig. 5a), perhaps because of the downregulation of receptor at a higher REF-1 concentration.

The growth-promoting activities of other relevant cytokines, TFPI-1, CNTF, and bFGF on RPE cells were compared at a 10-ng/mL concentration. TFPI-1 is a member of the TFPI family with 35% amino acid sequence homology with TFPI-2; however, RPE cells did not respond to TFPI-1. CNTF, a human ciliary nerve nutritional factor, also did not stimulate RPE cell proliferation. However, the growth stimulation of bFGF was stronger than that of REF-1 (Fig. 5b).

Growth stimulation of HUVECs, human fibroblasts, rabbit primary RPE cells, and fourth-passage human primary RPE cells was also examined (Fig. 5c). A 12% and 25% increase after

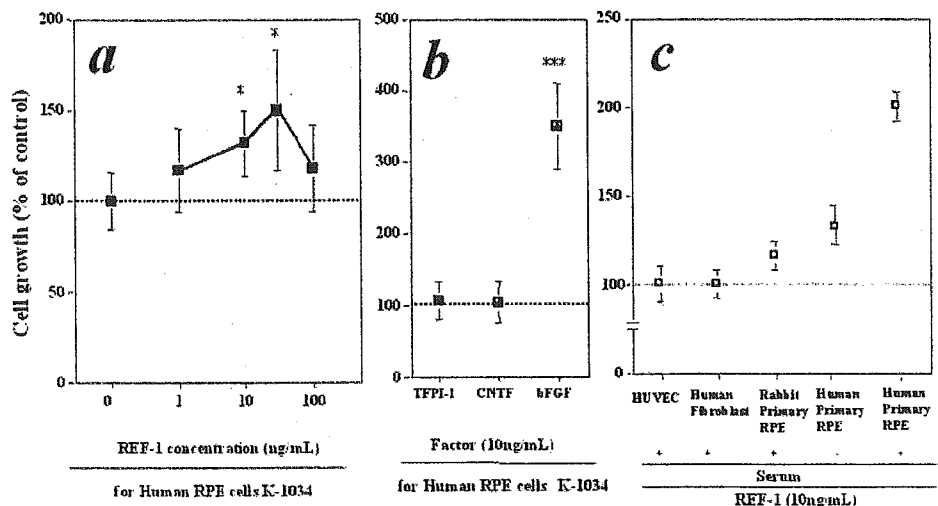
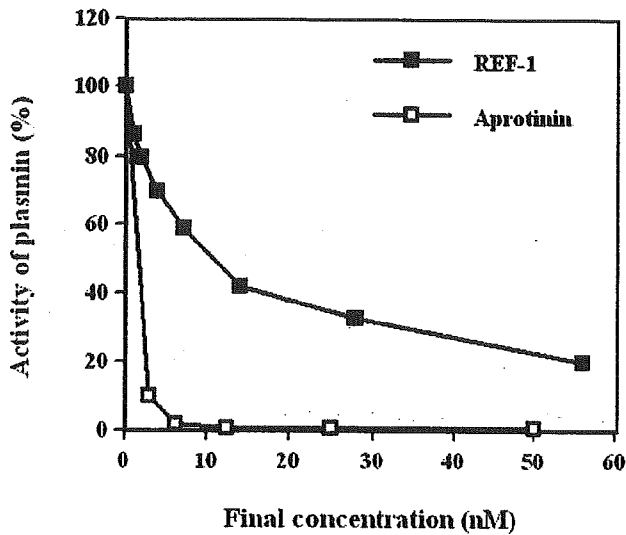


FIGURE 5. Cell proliferation activity of recombinant REF-1. Dose-dependent REF-1 activity in human K-1034 RPE cells (a), growth-promoting activities of TFPI-1, CNTF, and bFGF in human K-1034 RPE cells (b), and proliferative response of HUVECs, human fibroblast, rabbit primary RPE cells, and human primary RPE cells to 10 ng/mL REF-1 (c).





**FIGURE 6.** Protease inhibitory activity of REF-1. The residual activities of plasmin with aprotinin (positive control, 4  $\mu\text{g}/\text{mL}$ ) or REF-1/TFPI-2 (5  $\mu\text{g}/\text{mL}$ ) were determined, in 96-well plastic plates, with S-2251 (Val-Leu-Lys-pNA, 1 mg/mL) used as a substrate. The percentage of relative activity in the inhibitor concentration was calculated from absorbance at 405 to 450 nm.

stimulation by REF-1 was observed in rabbit primary RPE cells and human primary RPE cells, respectively. Significant proliferation was observed in human primary RPE cells cultured in medium with 15% FCS.

**Proteinase Inhibitory Activity**

REF-1 inhibited plasmin (Fig. 6), and it was confirmed that it inhibited serine protease.

**Determination of REF-1 in Human Primary RPE Cells**

The existence of REF-1 was determined in human primary RPE cells by Western blot analysis and RT-PCR (Fig. 7). REF-1 was

not detected in RPE cells by Western blot under the conditions we used; however, REF-1 mRNA was detected in total RNA extracted from human primary RPE cells by 30 cycles of PCR.

**Effect of REF-1 Treatment on Cytokine Production of RPE Cells**

Eleven cytokines and growth factors were measured in serum-free culture medium of fourth-passage human primary RPE cells treated with 10 ng/mL of REF-1 for 2 days. TGF- $\beta$ 1 and GM-CSF were significantly induced by 4.7- and 2.4-fold, respectively. bFGF, IL-6, IL-8, and M-CSF showed no or only a moderate increase with REF-1 treatment. TGF- $\beta$ 2, IL-1 $\beta$ , G-CSF, TNF- $\alpha$ , and EGF were undetectable (Table 2).

**DISCUSSION**

We have isolated and identified a biologically active protein that stimulated RPE cell to proliferate and consider it to be a potential therapeutic agent. This factor has growth-promoting properties that it exerts on RPE cells and was identified as REF-1 protein. Molecular cloning showed that this factor was homologous to the TFPI-2/PP5 protein. The RPE cell growth-promoting effect of REF-1/TFPI-2 was found to be more specific to RPE cells than to fibroblasts and HUVECs. Currently, there are no reports of factors that specifically stimulate the growth of RPE cells, although several growth factors such as bFGF, EGF, PDGF, and VEGF are growth promoters. These factors also have other properties, such as angiogenesis and potential stimulation of endothelial cell growth and can cause proliferative vitreoretinopathy by fibroblast proliferation. These undesirable properties do not allow them to be used for the treatment of retinal diseases. Although REF-1/TFPI-2 has a relatively weaker growth-promoting action than bFGF in vitro, it did not stimulate endothelial cell growth or fibroblast proliferation. Thus, the specificity of REF-1/TFPI-2 to RPE cells is greater than that of other growth factors (Fig. 5).

We determined the growth-promoting activity of REF-1/TFPI-2 using 10th- to 20th-passage human K-1034 RPE cells, primary HUVECs, primary rabbit RPE cells, and 4th-passage primary human RPE cells. Early-passage RPE cells responded

**Determination of REF-1 in RPE Cells by Western Blotting Analysis and RT-PCR**

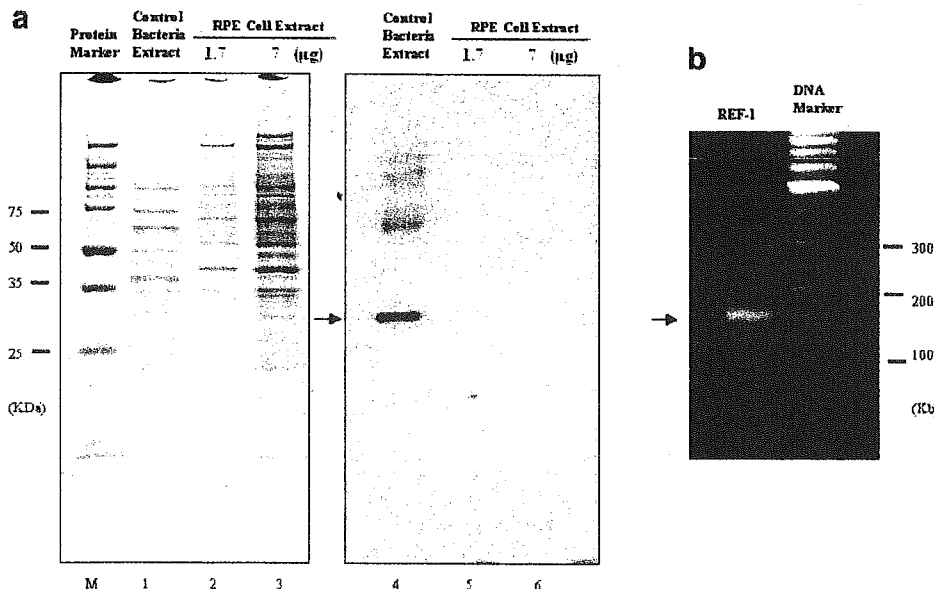


**FIGURE 7.** Determination of REF-1 in human primary RPE cells. REF-1 in human primary RPE cells was determined by Western blot analysis or RT-PCR. (a) Western blot of REF-1 for human primary RPE cell extract. Lane 1: Coomassie staining of bacteria extract expressing recombinant REF-1 (34 kDa); lane 2: Coomassie staining of human RPE cell extract (1.7  $\mu\text{g}$ ); lane 3: Coomassie staining of RPE cell extract (7  $\mu\text{g}$ ); lane 4: Western blot of bacteria extract expressing recombinant REF-1 (34 kDa); lane 5: Western blot of RPE cell extract (1.7  $\mu\text{g}$ ); lane 6: Western blot of RPE cell extract (7  $\mu\text{g}$ ). (b) RT-PCR of REF-1 transcript in total RNA extracted from human primary RPE cells. A single band was observed after 30 cycles of amplification.

TABLE 2. Production of Cytokines by Human Primary RPE Cells Treated with REF-1 (10 ng/mL)

Cytokine	REF-1 (pg/10 <sup>5</sup> cells)		+/-
	-	+	
bFGF	508	546	1.0
TGF- $\beta$ 1	673	3163	4.7
TGF- $\beta$ 2	Nondetectable	Nondetectable	—
IL-1 $\beta$	Nondetectable	Nondetectable	—
IL-6	1770	1922	1.1
IL-8	556	837	1.5
G-CSF	Nondetectable	Nondetectable	—
GM-CSF	817	1959	2.4
M-CSF	420	509	1.2
TNF- $\alpha$	Nondetectable	Nondetectable	—
BGF	Nondetectable	Nondetectable	—

satisfactorily to REF-1; however, aged K-1034 RPE cells did not (data not shown), whereas primary rabbit RPE cells and primary HUVECs responded poorly to REF-1. Aged K-1034 RPE cells retained their response to basic FGF as well as early-passaged cells. These observations indicate that the growth-promoting effect of RPE-1 may be age-related and that it probably stimulates growth by a pathway different from that used by other growth factors such as bFGF. Although, growth stimulation was observed for human primary RPE cells in both serum-free and serum-added medium, REF-1 favored the latter condition, resulting in fourfold proliferation. Exogenous factor(s) may be involved in this effect.

Our experiments showed that at least 2 of 11 cytokines were stimulated by REF-1 treatment. To our surprise, TGF- $\beta$ 1 production was significantly induced (4.7-fold) in REF-1-treated compared with nontreated cells. A possible explanation for this phenomenon is that TGF- $\beta$ 1 production is stimulated to suppress and balance the rapid growth rate of RPE cells. This suggestion may be supported by the inhibitory effect of TGF- $\beta$ 1 on RPE cell proliferation.<sup>21</sup>

Another cytokine, increased by 2.4-fold, was colony-stimulating factor GM-CSF. GM-CSF is known to be an important regulator of macrophage, granulocyte, dendritic cell, and eosinophil behavior.<sup>22,23</sup> RPE cells have properties similar to macrophages—that is, to phagocytose and generate different cytokines, including GM-CSF.<sup>24</sup> In RPE cells, GM-CSF has been reported to be upregulated in response to TNF- $\alpha$ ,<sup>24</sup> IL-1 $\alpha$ ,<sup>25</sup> or IL-1 $\beta$ <sup>26</sup> and downregulated by IFN- $\gamma$ .<sup>26</sup> The signal transduction mechanism for upregulation of GM-CSF by REF-1 is currently under investigation.

REF-1 was detected by RT-PCR in human primary RPE cells after 30 cycles of PCR; however, Western blot analysis failed to detect REF-1 in the experimental conditions we used. REF-1 mRNA may require specific stimulation to produce protein in RPE cells.

TFPI-2 has been shown to act as an anticoagulant<sup>8</sup> and serine protease inhibitor.<sup>9</sup> It is unclear whether these activities are correlated with growth promotion. Recent studies on TFPI-2 have shown that it has novel biological effects, such as inhibition of matrix metalloproteinase (MMP),<sup>15,16</sup> promotion of smooth muscle growth,<sup>17</sup> and modulation of melanoma and glioma invasion.<sup>18,19</sup> The relationship between these activities and promotion of RPE cell proliferation is still unknown. TFPI-2/REF-1 has been found in human ciliary epithelium<sup>20</sup> and may play an important role in the normal RPE environment. It also has potential for therapeutic use for ocular tissue damage. To confirm these possibilities further pharmacological evaluations in vivo are needed, using suitable animal models and effective drug delivery methods to the damaged sites.

## References

- Marmor MF. Introduction to structure, function, and diseases of the retinal pigment epithelium. In: Marmor MF, Wolfensberger TJ. *The Retinal Pigment Epithelium: Function and Disease*. London, UK: Oxford University Press. 1998;3-12.
- Hackett SF, Schoenfeld CL, Freund J, Gottsch JD, Bhargava S, Campochiaro PA. Neurotrophic factors, cytokines and stress increase expression of basic fibroblast growth factor in retinal pigmented epithelial cells. *Exp Eye Res*. 1997;64:865-873.
- Campochiaro PA, Glaser BM. Platelet-derived growth factor is chemotactic for human retinal pigment epithelial cells. *Arch Ophthalmol*. 1985;103:576-579.
- Kaven CW, Spraul CW, Zavazava NK, Lang GK, Lang GE. Growth factor combinations modulate human retinal pigment epithelial cell proliferation. *Curr Eye Res*. 2000;20:480-487.
- Schweigerer L, Neufeld G, Friedman J, Abraham JA, Fiddes JC, Gospodarowicz D. Capillary endothelial cells express basic fibroblast growth factor, a mitogen that promotes their own growth. *Nature*. 1987;325:257-259.
- Cassidy L, Barry P, Shaw C, Duffy J, Kennedy S. Platelet derived growth factor and fibroblast growth factor basic levels in the vitreous of patients with vitreoretinal disorders. *Br J Ophthalmol*. 1998;82:181-185.
- Kliffen M, Sharma HS, Mooy CM, Kerkvliet S, de Jong PT. Increased expression of angiogenic growth factors in age-related maculopathy. *Br J Ophthalmol*. 1997;81:154-162.
- Sprecher CA, Kiesel W, Mathewes S, Foster DC. Molecular cloning, expression, and partial characterization of a second human tissue-factor-pathway inhibitor. *Proc Natl Acad USA*. 1994;91:3353-3357.
- Miyagi Y, Koshikawa N, Yasumitsu H, et al. cDNA cloning and mRNA expression of a serine proteinase inhibitor secreted by cancer cells: identification as placental protein 5 and tissue factor pathway inhibitor-2. *J Biochem*. 1994; 116:939-942.
- Utsumi J, Iizuka M, Kobayashi S. Interferon production with multitray culture system on a large scale. *J Interferon Res*. 1984;4:9-16.
- Kigasawa K, Souchi S, Tanaka Y, Obazawa H. Morphologic and chromosomal study of a human retinal pigment epithelial cell line. *Jpn J Ophthalmol*. 1994;38:10-15.
- Sano E, Okano K, Sawada R, et al. Constitutive long-term production and characterization of recombinant human interferon-gammas from two different mammalian cells. *Cell Struct Funct*. 1988; 13:143-159.
- Petersen LC, Sprecher CA, Foster DC, Blumberg H, Hamamoto T, Kiesel W. Inhibitory properties of a novel human Kunitz-type protease inhibitor homologous to tissue factor pathway inhibitor, *Biochemistry*. 1996;35:266-272.
- Rao CN, Reddy P, Liu Y, et al. Extracellular matrix-associated serine protease inhibitors (Mr. 33, 000, 31,000, and 27, 000) are single-gene products with differential glycosylation: cDNA cloning of the 33-kDa inhibitor reveals its identity to tissue factor pathway inhibitor-2. *Arch Biochem Biophys*. 1996;335:82-92.
- Rao CN, Mohanam S, Puppala A, Rao JS. Regulation of proMMP-1 and proMMP-3 activation by tissue factor pathway inhibitor-2/matrix-associated serine protease inhibitor. *Biochem Biophys Res Commun*. 1999;255:94-98.
- Herman MP, Sukhova GK, Kiesel W, et al. Tissue factor pathway inhibitor-2 is a novel inhibitor of matrix metalloproteinases with implication for atherosclerosis. *J Clin Invest*. 2000;107:1117-1126.
- Shinoda E, Yui Y, Hattori R, et al. Tissue factor pathway inhibitor-2 is a novel mitogen for vascular smooth muscle cells. *J Biol Chem*. 1999;274:5379-5384.
- Konduri SD, Tasiou A, Chandrasekar N, Nicolson GL, Rao JS. Role of tissue factor pathway inhibitor-2 (TFPI-2) in amelanotic melanoma (C-32) invasion. *Clin Exp Metastasis*. 2000;18:303-308.
- Konuri SD, Rao CN, Chandrasekar N, et al. A novel function of tissue factor pathway inhibitor-2 (TFPI-2) in human glioma invasion. *Oncogene*. 2001;20:6938-6945.

20. Ortego J, Escribano J, Coca-Prados M. Gene expression of proteases and protease inhibitors in the human ciliary epithelium and ODM-2 cells. *Exp Eye Res.* 1997;65:289-299.
21. Lee SC, Seong GJ, Kim SH, Kwon OW. Synthesized TGFbeta s in RPE regulates cellular proliferation. *Kor J Ophthalmol.* 1999;13:16-24.
22. Gasson JC. Molecular physiology of granulocyte-macrophages colony stimulating factors. *Blood.* 1991;77:1131-1145.
23. Fischer HG, Frosch S, Reske K, Reske-Kunz AB. Granulocyte-macrophages colony-stimulating factor activates macrophages derived from bone marrow cultures to synthesis of MHC class II molecules and to augmented antigen presentation. *J Immunol.* 1988;141:3882-3888.
24. Crane IJ, Kuppner MC, McKillop-Smith S, Wallace CA, Forrester JV. Cytokine regulation of granulocyte-macrophage colony-stimulating factor (GM-CSF) production by human retinal pigment epithelial cells. *Clin Exp Immunol.* 1999;115:288-293.
25. Plank SR, Huang X-N, Robertson JE, Rosenbaum JT. Retinal pigment epithelial cells produce interleukin-1 $\beta$  and granulocyte-macrophage colony-stimulating factor in response to interleukin-1 $\alpha$ . *Curr Eye Res.* 1993;12:205-212.
26. Crane IJ, Wallace CA, Forrester JV. Regulation of granulocyte-macrophage colony-stimulating factor in human retinal pigment epithelial cells by IL-1 $\beta$  and IFN- $\gamma$ . *Cell Immunol.* 2001;209:132-139.



# Bio Medical Quick Review Net

No. 4001

## インベーター法を用いた緑内障の遺伝子解析

岩田 岳<sup>1</sup>・真島 行彦<sup>2</sup>

国立病院東京医療センター臨床研究センター細胞・分子生物学研究室 室長<sup>1</sup>  
慶應義塾大学医学部眼科学教室 助教授<sup>2</sup>

株式会社メディカル ドウ

Medical Do Co., Ltd.

本Reviewの内容を無断で複製、転載すると、著作権、出版権侵害となる場合がありますのでご注意ください。

# インベーター法を用いた緑内障の遺伝子解析

岩田 岳<sup>1</sup>・真島 行彦<sup>2</sup>

国立病院東京医療センター臨床研究センター細胞・分子生物学研究室 室長<sup>1</sup>  
慶應義塾大学医学部眼科学教室 助教授<sup>2</sup>

緑内障は通常、眼圧の上昇により視神経が圧迫され、視神経萎縮をきたし、放置すると視野欠損を生じ、最後には失明にいたる眼疾患である。われわれは緑内障の早期診断・早期治療を目指し、遺伝性の緑内障に限って遺伝子変異や遺伝子多型を簡単に解析できる「緑内障遺伝子診断プレート」のプロトタイプを米国Third Wave社が開発したインベーター法（国内ではBML社が販売）を用いて完成させ、簡単な操作で多数の検体について既知の遺伝子変異あるいは遺伝子多型の検出が可能になった。本稿では眼科の分野で研究が遅れている遺伝子診断技術についてインベーター法を中心に考察する。

key  
words

緑内障、眼圧、視神経、神経乳頭、遺伝子診断、遺伝子変異、  
遺伝子多型、PCR、蛍光プレートリーダー、インベーター法

## はじめに

緑内障は「視神経乳頭、視野の特徴的変化の少なくとも1つを有し、通常、眼圧を十分に下降させることにより視神経障害の改善あるいは進行を防止しうる眼の機能的構造異常を特徴とする疾患」と定義される（日本眼科学会誌107巻3号）、通常眼圧の上昇により視神経が圧迫され視神経萎縮をきたし、放置すると視野欠損を生じ、最後には失明にいたる眼疾患である。日本人成人の失明原因としては第2位の疾患である。40歳以上の有病率は約5%で、年齢

とともに有病率は増加しており、日本においては約200万人の患者が存在すると推測されている。しかしながら、緑内障患者は自覚症状が乏しいため、眼科を受診しているのはその1/3に過ぎない。眼圧上昇との関連性が長年示唆されてきたが、最近の調査によって、日本人には正常な眼圧をもちながら疾患にいたる患者が多数存在することが明らかとなり、視野検査、眼底検査、そして眼圧測定だけでは疾患の早期発見が難しい。

緑内障は、遺伝的要素と環境的因子の双方が発症に関係している多因子疾患（または多遺伝子疾患）

Takeshi Iwata<sup>1</sup>・Yukihiko Mashima<sup>2</sup>

Laboratory of Cellular & Molecular Biology, National Institute of Sensory Organs, National Tokyo Medical Center,  
Laboratory Chief<sup>1</sup>

Department of Ophthalmology, School of Medicine, Keio University, Associate professor<sup>2</sup>

Molecular diagnostic of glaucoma using Invader technology

E-mail: iwataakeshi@kankakuki.go.jp

表1 緑内障遺伝子の染色体マッピング

遺伝子座	染色体部位	遺伝子	緑内障の型	遺伝形式	診断年齢(歳)
GLC1A	1q23-25	MYOC	JPOAG	常優	5~77
GLC1B	2cen-q13	不明	POAG	常優	>40
GLC1C	3q21-24	不明	POAG	常優	>40
GLC1D	8q23	不明	POAG	常優	
GLC1E	10p15-14	OPTN	NTG	常優	23~65
GLC1F	7q35-36	不明	POAG	常優	25~70
GLC3A	2p21	CYP1B1	PCG	常劣	<3
GLC3B	1p36	不明	PCG	常劣	<3

GLC1: 開放隅角緑内障, GLC2: 閉塞隅角緑内障, GLC3: 先天緑内障  
 JPOAG: Juvenile primary open-angle glaucoma 若年性開放隅角緑内障  
 POAG: Primary open-angle glaucoma 開放隅角緑内障  
 NTG: Normal-tension glaucoma 正常眼圧緑内障  
 PCG: Primary congenital glaucoma 先天緑内障  
 (Human Genome Organization/Genome Database Nomenclature Committeeによる  
 GLC分類)

と考えられている。現在、緑内障の危険因子として明らかなのは高眼圧と家族歴である。以前から、緑内障患者の30~50%に家族性のものがあることが広く知られていた。疫学調査で緑内障発症の相対危険度は、近親に緑内障患者がいると2.85倍と報告されている。緑内障患者のうち、実際に眼科を受診しているのはその1/3に過ぎないという現状を考えると、遺伝子検査により遺伝子変異が検出されれば、発症前に緑内障発症の危険因子を知ることになり、今後の管理・治療・予防の点で有用な情報となりうるということが期待される。

今回われわれは緑内障の早期診断・早期治療を目指し、遺伝性の緑内障に限って遺伝子変異や遺伝子多型を簡単に解析できる「緑内障遺伝子診断プレート」のプロトタイプを米国Third Wave社が開発したInvader法(国内ではBML社が販売)を用いて完成させ、簡単な操作で多数の検体について既知の遺伝子変異あるいは遺伝子多型を解析することが可能となった。本稿では眼科の分野で研究が遅れている遺伝子診断技術についてインベーター法を中心に考察する。

## 1. 緑内障の原因遺伝子

緑内障は大きく原発開放隅角緑内障, 原発閉塞隅角緑内障, 先天性緑内障に分類されているが、このなかには遺伝的な原因によって生じるものが約20%含まれており、開放隅角緑内障の明らかな発症因子ともいべき緑内障遺伝子(常染色体優性遺

伝形式)は、現在少なくとも6個その存在が染色体上に確認されている(表1)。このうち3つの遺伝子が同定されており、原因が特定できる緑内障として世界中で盛んに研究が行われている。

### 1. ミオシリン(Myocilin: MYOC)

緑内障発症の直接的な原因は長年不明のままであったが、1997年Stoneらによって、それまでTIGR(タイガー)と呼ばれていた線維柱帯細胞で発見されたステロイド感受性のタンパク質が開放隅角緑内障の原因であることが報告された。後に窪田らがクローニングしたミオシリン(Myocilin)遺伝子

と同一のものであることが判明し、遺伝子名登録機関であるHUGOに登録済みであったが、ミオシリンが正式な遺伝子名として定着した。ミオシリンによる発症は、特に若年(35歳以前)の開放隅角緑内障患者に比較的多く(約36%)遺伝子変異がみられるが、全年代を含めた開放隅角緑内障患者では約4%に遺伝子変異がみられる。表2に、日本人緑内障患者に報告されたミオシリン変異を記載した。

### 2. チトクロームP4501B1(CYP1B1)

先天異常である先天緑内障は常染色体劣性遺伝形式で、多くは出生時、または少なくとも出生後1年以内に発症する疾患である。原発先天緑内障に関しては、1番染色体と2番染色体の2ヵ所に疾患遺伝子(それぞれGLC3BとGLC3A)が存在しており、GLC3Aは1997年に薬物代謝酵素関連のチトクロームP4501B1(遺伝子記号はCYP1B1)が明らかになった。先天緑内障の発症頻度は、欧州では5000人から22000人に1人、中近東では2500人に1人、スロバキアのジブシーでは1250人に1人と、地域によりかなり異なる。中近東やスロバキアのジブシーでは、先天緑内障が失明の上位を占める。日本においては、先天緑内障の発症頻度は不明である。先天緑内障の多くは家族歴がみられないが、約10%に常染色体劣性遺伝の家系が報告されている。外国では両親が血族結婚でみられることが多いが、日本において現在血族結婚はまれであり、両親が異なる変異をもつ保因者である場合がほとんどである。

われわれは、日本人の先天緑内障患者における

表2 日本人開放隅角緑内障のMYOC変異

変異	診断時年齢(歳)	家族歴	文献
Ile 360 Asn	59	+	日眼 106 : 201, 2002
Ala 363 Thr	32	+	Hum Mut 16 : 270, 2000
Gly 367 Arg	29,36,45	+	Jpn J Ophthalmol 44 : 445, 2000
Pro 370 Leu	13,26	+	Jpn J Ophthalmol 43 : 80, 1999
Thr 448 Pro	32,35,42	+	Jpn J Ophthalmol 43 : 85, 1999
Ile 465 Met	?	?	Hum Mol Gen 8 : 899, 1999
多型の可能性		文献	
Arg 46 Stop	Hum Mut 16 : 270, 2000	Clin Genet 59 : 263, 2001	
Arg 158 Gln	Hum Mut 16 : 270, 2000	Clin Genet 59 : 263, 2001	
Asp 208 Glu	Hum Mut 16 : 270, 2000	Clin Genet 59 : 263, 2001	
Thr 353 Ile	Hum Mol Gen 8 : 899, 1999	IOVS 41 : 1386, 2000	
Pro 481 Ser	Clin Genet 59 : 263, 2001		

表3 日本人の先天緑内障患者にみられたCYP1B1遺伝子変異(文献1より)

家系数	塩基変化(塩基番号)	アミノ酸変化(コドン番号)
3	4776 insAT/G7927A	Frameshift/ Val 364 Met
1	A4380T/A4380T	Asp 192 Val/Asp 192 Val
1	A4380T/G7927A	Asp 192 Val/Val 364 Met
1	G4793T, C4794T/G7927A	Ala 330 Phe/Val 364 Met
1	G7927A/G8168A	Val 364 Met/Arg 444 Gln
1	3964 del C/G8168A	Frameshift/Arg 444 Gln
1	C4645A/G8168A	Cys 280 stop/Arg 444 Gln
2	C3130T/G4763T	Unknown/Val 320 Leu
1	G4397A/Unidentified	Val 198 Ile/Unidentified
1	A8333G/Unidentified	Glu 499 Gly/Unidentified

13家系

表4 緑内障遺伝子OPTN変異(文献2より)

Exon		Glaucoma	Normal
4	Glu 50 Lys	7/52 (13.5%)	0/540
6	InsAG (Premature stop)	1/46 (2.2%)	0/200
16	Arg 545 Gln	1/46 (2.2%)	0/100
危険因子			
5	Met 98 Lys	23/169 (13.6%)	9/422 (2.1%)

CYP1B1遺伝子変異を検討したが、65家系中13家系(20%)に日本人特有の11種類の新しい変異が確認された(表3)。今回の日本人患者では血縁結婚はみられず、13家系中ホモ変異は1家系のみであり、ほかは複合ヘテロ変異であった。興味あることに、11種類の変異のうち、Val364Met変異は9人中6人に確認された。ハプロタイプは調べていないが、同一の祖先から出てきた可能性(創始者変異)も考えられる。

### 3. オプチニューリン

(Optineurin : OPTN)

2002年に発見された最も新しい緑内障遺伝子としてオプチニューリン(遺伝子記号はOPTN)がある。米国では家族性の正常眼圧緑内障家系の17%に遺伝子異常がみられたと報告されている(表4)。この遺伝子についての最初の論文では複数の遺伝子変異が報告されていたが、世界中でこれを追試した結果、アミノ酸番号50番の変異と核酸番号691番の2塩基挿入による変異以外はすべて正常者にも観察されるアミノ酸の変化を伴う遺伝子多型であることが判明した。最近の報告では日本人緑内障患者の300人に1名しか、この遺伝子に変異がないことが報告されている。しかしながら、この遺伝子の変異によって確実に正常眼圧緑内障が発症することから、患者数の多いわが国で詳細な研究が望まれている。

### 4. その他の緑内障遺伝子

開放隅角緑内障において少なくとも6個の緑内障遺伝子が存在するということは、緑内障患者の30~40%は遺伝的要因が強いといえる。若年発症の開放隅角緑内障患者でミオシリン遺伝子変異をもつ家系では、家族内での発症患者は、メンデルの遺伝形式に従い約50%の発症率がみられる。しかしながら、40歳以降に発症した開放隅角緑内障患者でミオシリン遺伝子変異をもっているにもかかわらず発症しない人もいて、発症には環境因子や遺伝子多型が影響する場合も考えられる。

## II. 緑内障の遺伝子診断

### 1. 感覚器臨床研究センターの発足

国立病院東京医療センター・臨床研究センターは感覚器疾患の専門研究機関として2003年度に発足し、研究事業の一環として慶應義塾大学医学部眼科学教室と共同で遺伝子診断システムの構築を開始した。全国から集まる多数のDNA検体について、これを解析するためには、これまでに利用し

てきたSSCP (single strand conformation polymorphism) 法やダイレクトシーケンス法をベースにした方法では、労働力、時間、コストの面で不相当と考えた。既知遺伝子変異あるいは既知遺伝子多型を正確にそして迅速に検出する新たな方法を市場で紹介されている技術の中から選択することにした。

## 2. 市場で紹介された主な遺伝子診断法

遺伝子診断システムについては市場で多数紹介されている方法をすべて検討し、そのなかから将来的に有効と思われる方式について、さらに検出感度、工程数、検出装置の価格、試薬の価格、試薬の安定性、新たな遺伝子変異・多型の追加の容易性、他疾患での診断実績、受託サービスを含む販売会社のサポート体制などについて検討を行った。現在市場には多数の遺伝子変異検出法が紹介されているが [GeneChip (Affymetrix社), Invader (Third Wave Technologies社), Sniper (Amersham Biosciences社), SNP-IT (Orchid Bioscience社), TaqMan-PCR (Applied Biosystems社), Pyro Sequencing (Pyrosequencing AB社), DNA Mass Array (Sequenom社), MALDI-TOF (Bruker社), ECA Chip (TUM研究所), Dynamic Allele Specific Hybridization (Thermo Electron Corporation社)], 評価の対象となった検出法は実績があり、一般の病院に普及させることを考えて、検出器の価格が1千万円を超えるものについては対象外とした。

### (1) 一塩基伸長法による遺伝子解析

ガラススライドにオリゴDNAをスポットして一塩基伸長法によって遺伝子変異を検出する方法としては、Asper Biotech社 (www.asperbio.com) のAPEX法やOrchid Biosciences社 (www.orchid.com) のSNP-IT法などがある。特にSNP-IT法は384穴プレートからガラススライドまで検体数に応じて複数の支持体を利用することができる。販売当初は桑和貿易からキットや検出器の販売が行われたが、現在は受託サービスのみとなっている。APEX法の特徴としては、スライドをエストニア (旧ソ連) で製造しているために安い人件費と高い技術力で先進国よりもコストが安く抑えられている。1万以上の変異オリゴDNAを1枚のスライドガラス上に

スポットして検出することに成功している。

### (2) WAVEによる遺伝子解析

Transgenomic社 (www.transgenomic.com) が販売する液体クロマトグラフィー (denaturing high performance liquid chromatography: DHPLC) を基本とした検出法である。ヘテロタイプの遺伝子変異である場合、患者DNAのPCR産物をいったん一本鎖に分離して再びハイブリダイゼーションさせたときに生じるヘテロドゥプレックスについて温度を調整しながら逆相カラムで分離することにより、部分的に解離した二本鎖DNAがその塩基配列に特有なパターンで分離される。PCR産物を液体クロマトグラフィーに流すだけなので、紹介する検出法のなかでは最も維持費がかからない方法である。未知遺伝子変異や遺伝子多型の検出に特に適しているが、変異の塩基配列の情報はSSCPと同様に得られない。

### (3) 一分子蛍光検出法による遺伝子解析

一分子蛍光検出法 (single molecule fluorescence detection) は蛍光励起用のレーザー光を開口数の大きな対物レンズで細く絞り、試料中に点状の微小光照射領域を作り、試料の濃度を調整することによって、この微小領域に1つの蛍光標識した分子しか観察できないようにする。この分子はブラウン運動によって激しく振動するが、これに他の分子を結合すると分子量が増加し、振動数が大幅に減少する。蛍光標識されたオリゴDNAと患者DNAのPCR産物が相補的に結合すると、ブラウン運動が鈍化し、結合したことが検出される。この方法はDNA検体のPCRを必要とするが、遺伝子変異あるいは遺伝子多型別に用意されたオリゴDNAとPCR産物を混合するのみで検出が可能であるため、大量の検体を同時に解析することが可能である。この方法を開発したノバスジーン社 (www.novus-gene.co.jp) は検出器と検出キットの販売だけでなく、受託サービスも行っている。

### (4) インベーター法による遺伝子解析

インベーター法は唯一PCRを不要とする遺伝子検出法で、米国 Third Wave Technologies社 (www.twt.com) が開発した方法である。遺伝子変異の塩基配列をもつインベーターオリゴDNAとブ



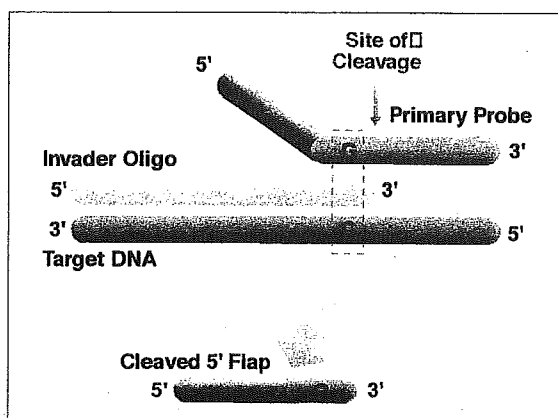


図1 インベーターオリゴDNAとプライマリープローブDNAがターゲットDNAと三重らせんを形成し、フラップが切断される

プライマリープローブオリゴDNAそしてゲノムDNAが複雑に96穴ウェル内で反応して、3重らせんDNAを形成し、これを認識してプライマリープローブが切断される(図1)。切断されて遊離したプライマリープローブはFRETカセットと呼ばれるオリゴDNAと結合して再び3重らせんDNAを形成する(図2)。FRETカセットには蛍光と蛍光を吸収するクエンチャーが近接しており、蛍光がクエンチャーによって吸収されるために発光しないが、3重らせんDNAが再び形成されると蛍光とクエンチャーの間が切断されて蛍光が遊離され、クエンチャーの影響を受けなくなるために発光が観察されるようになる。反応に必要な検体DNAと水以外の各種オリゴDNAと酵素類は乾燥した状態で各ウェルの底に封入して保存することができる。このために疾患別あるいは遺伝子別に診断用96穴プレートを作製して、測定時にプレートを開封して検体DNAと水を加えるだけで解析することができる。

### III. インベーター法検出プロトコール

インベーター法の具体的な操作法は図3のとおりである。インベーター法による臨床検査についてはBML社が国内販売権を所有している。われわれは、この方式に基づいて緑内障遺伝子ミオシリン、チトクロムP4501B1およびオプチニューリンについて、日本人で発見された合計20の遺伝子変異を選択して、これを検出する世界で初めての緑

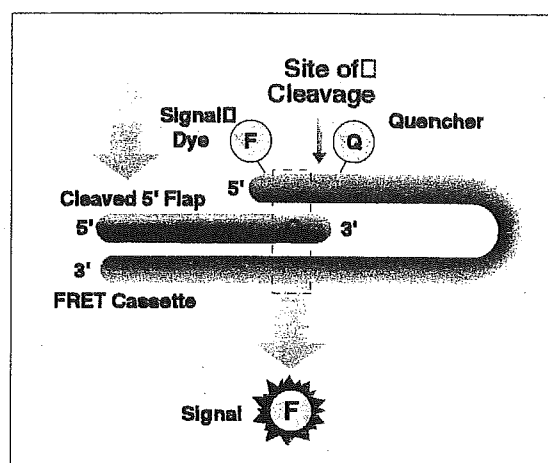


図2 切断されたフラップDNAはFRETカセットDNAと三重らせんを再び形成して切断されて蛍光色素とクエンチャーが離れて発光する

内障遺伝子診断用プレートの開発を行った。この開発については2003年7月に日経バイオテックなどで報道され、多くの臨床医の先生方に興味をもっていただいたが、インベーター法や一塩基伸長法にも欠点は存在する。それはオリゴDNAと患者DNAが結合する際に、オリゴDNAの範囲内に変異が存在した場合には結合が不十分なために反応が起こらず、結果が得られないことである。この問題を解決するために、遺伝子エクソン内のすべての塩基配列について検出できるようにプローブを作製しなければならない。

### おわりに

最近、岐阜県多治見市(人口106,000人)で行われた、日本緑内障学会多治見市疫学調査による受診者の調査(3021人、参加率78%)によると、40歳以上の5.8%にあたる人が原発開放隅角緑内障であることが判明し、このなかで正常眼圧緑内障が60%以上と、世界的にも類をみないほど正常眼圧の患者が多いことが判明した。視野測定、眼圧測定そして眼底観察などの診断に加えて遺伝子診断が簡単に行えるようになれば、今後の診断に大いに助けとなると考えられる。しかしながら、癌や糖尿病など患者数の多い国民病については順調に遺伝子診断法の開発が行われているが、眼科の分野については企業側の情報不足によってその重要

図3 インベーター法のプロトコール (96well Wet Format)

1. Invader Biplax 96-well Plateのレイアウトを決める (次ページ参照)																			
2. ゲノムDNAを95℃で10分間インキュベートする																			
3. Probe/Cleavase/MgCl2 mixを作る																			
<table border="1"> <tr> <th>Solution</th> <th>1反応あたりの量 (ul)</th> </tr> <tr> <td>PPI mix</td> <td>3.0</td> </tr> <tr> <td>FRET Buffer</td> <td>3.5</td> </tr> <tr> <td>Cleavase XI / MgCl2</td> <td>1.0</td> </tr> <tr> <td>Total</td> <td>7.5</td> </tr> </table>		Solution	1反応あたりの量 (ul)	PPI mix	3.0	FRET Buffer	3.5	Cleavase XI / MgCl2	1.0	Total	7.5								
Solution	1反応あたりの量 (ul)																		
PPI mix	3.0																		
FRET Buffer	3.5																		
Cleavase XI / MgCl2	1.0																		
Total	7.5																		
4. 3で作った Probe/MgCl2 mixを Invader Biplax 96well Plateに7.5ul/well入れる																			
5. 2のゲノムDNAまたはコントロール用合成オリゴヌクレオチドをInvader Biplax 96well Plateに7.5ul/well (ゲノムDNA:15ng/ul,約100ng/7.5ul/well) 入れる																			
6. ミネラルオイルを Invader Biplax 96well Plateに15ul/well入れる																			
7. ヒートブロックまたはサーマルサイクラーで63℃で4時間インキュベートする																			
8. 蛍光プレートリーダーで以下の波長を用い測定する																			
<table border="1"> <tr> <th colspan="3">Wavelength/Bandwidth</th> </tr> <tr> <td rowspan="2">FAM</td> <td>Excitation</td> <td>485nm/20nm</td> </tr> <tr> <td>Emission</td> <td>530nm/25nm</td> </tr> <tr> <td rowspan="2">RED</td> <td>Excitation</td> <td>560nm/20nm</td> </tr> <tr> <td>Emission</td> <td>620nm/40nm</td> </tr> </table>		Wavelength/Bandwidth			FAM	Excitation	485nm/20nm	Emission	530nm/25nm	RED	Excitation	560nm/20nm	Emission	620nm/40nm					
Wavelength/Bandwidth																			
FAM	Excitation	485nm/20nm																	
	Emission	530nm/25nm																	
RED	Excitation	560nm/20nm																	
	Emission	620nm/40nm																	
9. 以下の基準で判定する																			
判定基準																			
<table border="1"> <thead> <tr> <th>判定</th> <th>Allelic Ratio</th> <th>FOZ</th> </tr> </thead> <tbody> <tr> <td>Allele 1 (FAM) Homozygous</td> <td><math>\geq 4.0</math></td> <td>FAM FOZ <math>\geq 1.6</math></td> </tr> <tr> <td>Equivocal-1</td> <td><math>&gt;2.5</math> to <math>&lt;4.0</math></td> <td></td> </tr> <tr> <td>Allele 1 and 2 Heterozygous FAM (RED) FOZ <math>\geq 1.3</math></td> <td></td> <td><math>\geq 0.4</math> to <math>\leq 2.5</math></td> </tr> <tr> <td>Equivocal-2</td> <td><math>&gt;0.25</math> to <math>&lt;0.4</math></td> <td></td> </tr> <tr> <td>Allele 2 (RED) Homozygous</td> <td><math>\leq 0.25</math></td> <td>RED FOZ <math>\geq 1.6</math></td> </tr> </tbody> </table>		判定	Allelic Ratio	FOZ	Allele 1 (FAM) Homozygous	$\geq 4.0$	FAM FOZ $\geq 1.6$	Equivocal-1	$>2.5$ to $<4.0$		Allele 1 and 2 Heterozygous FAM (RED) FOZ $\geq 1.3$		$\geq 0.4$ to $\leq 2.5$	Equivocal-2	$>0.25$ to $<0.4$		Allele 2 (RED) Homozygous	$\leq 0.25$	RED FOZ $\geq 1.6$
判定	Allelic Ratio	FOZ																	
Allele 1 (FAM) Homozygous	$\geq 4.0$	FAM FOZ $\geq 1.6$																	
Equivocal-1	$>2.5$ to $<4.0$																		
Allele 1 and 2 Heterozygous FAM (RED) FOZ $\geq 1.3$		$\geq 0.4$ to $\leq 2.5$																	
Equivocal-2	$>0.25$ to $<0.4$																		
Allele 2 (RED) Homozygous	$\leq 0.25$	RED FOZ $\geq 1.6$																	
$\text{Allelic Ratio} = \frac{(\text{FAM Raw Counts} / \text{FAM NTC Raw Counts}) - 1}{(\text{RED Raw Counts} / \text{RED NTC Raw Counts}) - 1}$ $= \frac{(\text{FAM FOZ}) - 1}{(\text{RED FOZ}) - 1}$ $= \frac{\text{NET FAM FOZ}}{\text{NET RED FOZ}}$																			

注) NET FAM (RED) FOZが、0以下のときはNET FAM (RED) FOZを0.01として計算する  
FOZ: Fold Over Zero, NTC: No Target Control

性が十分に知られておらず、開発が遅れている。

これまでに発見された多数の遺伝性眼疾患の変異については日本人と欧米人との比較が行われているが、位置やその頻度について異なる場合が多く、米国を中心とした遺伝子変異の情報が必ずしも日本人に当てはまらないケースが多い。今回構築中の症例登録システム、遺伝子診断システム、そしてデータベースシステムは日本人の遺伝子解析を目的としており、遺伝子診断システムについても日本人で発見された既知遺伝子変異や既知

遺伝子多型が中心となる。より多くの研究室そして診療病院で臨床医が正確にそして簡単に遺伝子解析ができることを目標に、利用可能な方式のなかからインベーター法を選択したが、この分野での進歩は凄まじいものがあり、より正確に、より少ないDNA量で、より早く、そして安価に解析できる装置が今後開発されていくと考えられる。

インベーター法は96穴プレート内の各ウェルがそれぞれ1変異に対応しており、塩基配列が一致した場合にのみ発光する、極めてわかりやすい測定法である。希釈した患者ゲノムDNAと水を加えて、反応を開始して、検出は簡単な蛍光プレートリーダーで検出することができる。この操作性の良さは自動化を可能とし、臨床の現場で使用できる診断装置に成長させることが期待される。

#### 参考文献

- 1) Mashima Y, et al : IOVS 42, 2211-2216, 2001.
- 2) Rezaie T, et al : Science 295, 1077-1079, 2002.
- 3) Izumi K, et al : Ophthalmic Res 35, 345-350, 2003.
- 4) Obazawa M, et al : IOVS (in press)

#### 著者プロフィール

岩田 岳:  
1988年名城大学農学部大学院博士課程卒業。1988年Visiting Fellow, National Eye Institute, NIH, 網膜色素変性症の連鎖解析を行う。1989年Research Associate, Bascom Palmer Eye Institute, 1991年Visiting Associate, National Eye Institute, NIH, 1995年Visiting Scientist, National Eye Institute, NIH, 糖尿病性網膜症に関するソルビトール経路 (アルドース還元酵素とソルビトール脱水素酵素) の転写・シグナル伝達の仕事に携わる。1999年~現在、国立病院東京医療センター臨床研究センター細胞・分子生物学研究室長。緑内障と加齢黄斑変性の原因解明と早期診断法の開発に力を注いでいる。今回紹介した研究内容は厚生労働省感覚器障害研究事業の一環として行われた。

## Proliferation of neural and neuronal progenitors after global brain ischemia in young adult macaque monkeys

Anton B. Tonchev,<sup>a</sup> Tetsumori Yamashima,<sup>a,\*</sup> Liang Zhao,<sup>a</sup>  
Hirotaka James Okano,<sup>b</sup> and Hideyuki Okano<sup>b</sup>

<sup>a</sup> Department of Neurosurgery, Division of Neuroscience, Kanazawa University Graduate School of Medical Science, Kanazawa 920-8641, Japan

<sup>b</sup> Department of Physiology, Keio University School of Medicine, Tokyo 160-8582, Japan

Received 3 September 2002; revised 13 December 2002; accepted 30 January 2003

### Abstract

To investigate the effect of global cerebral ischemia on brain cell proliferation in young adult macaques, we infused 5-bromo-2'-deoxyuridine (BrdU), a DNA replication indicator, into monkeys subjected to ischemia or sham-operated. Subsequent quantification by BrdU immunohistochemistry revealed a significant postischemic increase in the number of BrdU-labeled cells in the hippocampal dentate gyrus, subventricular zone of the temporal horn of the lateral ventricle, and temporal neocortex. In all animals, 20–40% of the newly generated cells in the dentate gyrus and subventricular zone expressed the neural progenitor cell markers Musashi1 or Nestin. A few BrdU-positive cells in postischemic monkeys were double-stained for markers of neuronal progenitors (class III  $\beta$ -tubulin, TUC4, doublecortin, or Hu), neurons (NeuN), or glia (S100 $\beta$  or GFAP). Our results suggest that ischemia activates endogenous neuronal and glial precursors residing in diverse locations of the adult primate central nervous system.

© 2003 Elsevier Science (USA). All rights reserved.

### Introduction

Generation of new neurons persists in the normal adult mammalian brain, with neural stem/progenitor cells residing in at least two brain regions: the subventricular zone (SVZ) of the lateral ventricle (Garcia-Verdugo et al., 1998) and the subgranular zone (SGZ) of the dentate gyrus (DG) (Gage et al., 1998). Adult neurogenesis is well-documented in the rodent, and has also been recently demonstrated *in vivo* in the normal DG of primates, including monkeys (Gould et al., 1999a; Kornack and Rakic, 1999) and humans (Eriksson et al., 1998). Neocortical neurogenesis in adult monkeys may exist (Gould et al., 1999b, 2001), but this issue remains controversial (Kornack and Rakic, 2001). Very recently, neurogenesis in the normal adult monkey

striatum and amygdala has been reported (Bedard et al., 2002; Bernier et al., 2002).

Brain injuries such as ischemia affect neurogenesis in adult rodents. Global ischemic insult enhances the proliferation of SGZ progenitors in gerbils (Liu et al., 1998), mice (Takagi et al., 1999), and rats (Kee et al., 2001; Yagita et al., 2001). Focal ischemia (Gu et al., 2000) or selective corticothalamic degeneration (Magavi et al., 2000) induces neurogenesis in the rodent neocortex. Focal ischemia also activates endogenous neuronal precursors in the rodent striatum (Arvidsson et al., 2002). However, whether an injury-triggered activation of endogenous neuronal precursors also takes place in the adult primate brain has not been addressed.

Here we investigated whether transient global ischemia in young adult monkeys affects the proliferation of neural progenitors and neuronal cells in DG and inferior temporal neocortex (IT), a neocortical area where adult neurogenesis under normal conditions was previously reported (Gould et al., 1999b, 2001). Young adults were specifically focused because neurogenesis decreases with age, in both the rodent (Kuhn et al., 1996) and monkey (Gould et al., 1999a).

\* Corresponding author. Department of Neurosurgery, Division of Neuroscience, Kanazawa University Graduate School of Medical Science, Takaramachi 13-1, Kanazawa city, 920-8641, Japan. Fax: +81-76-234-4262.  
E-mail address: [yamashim@med.kanazawa-u.ac.jp](mailto:yamashim@med.kanazawa-u.ac.jp) (T. Yamashima).

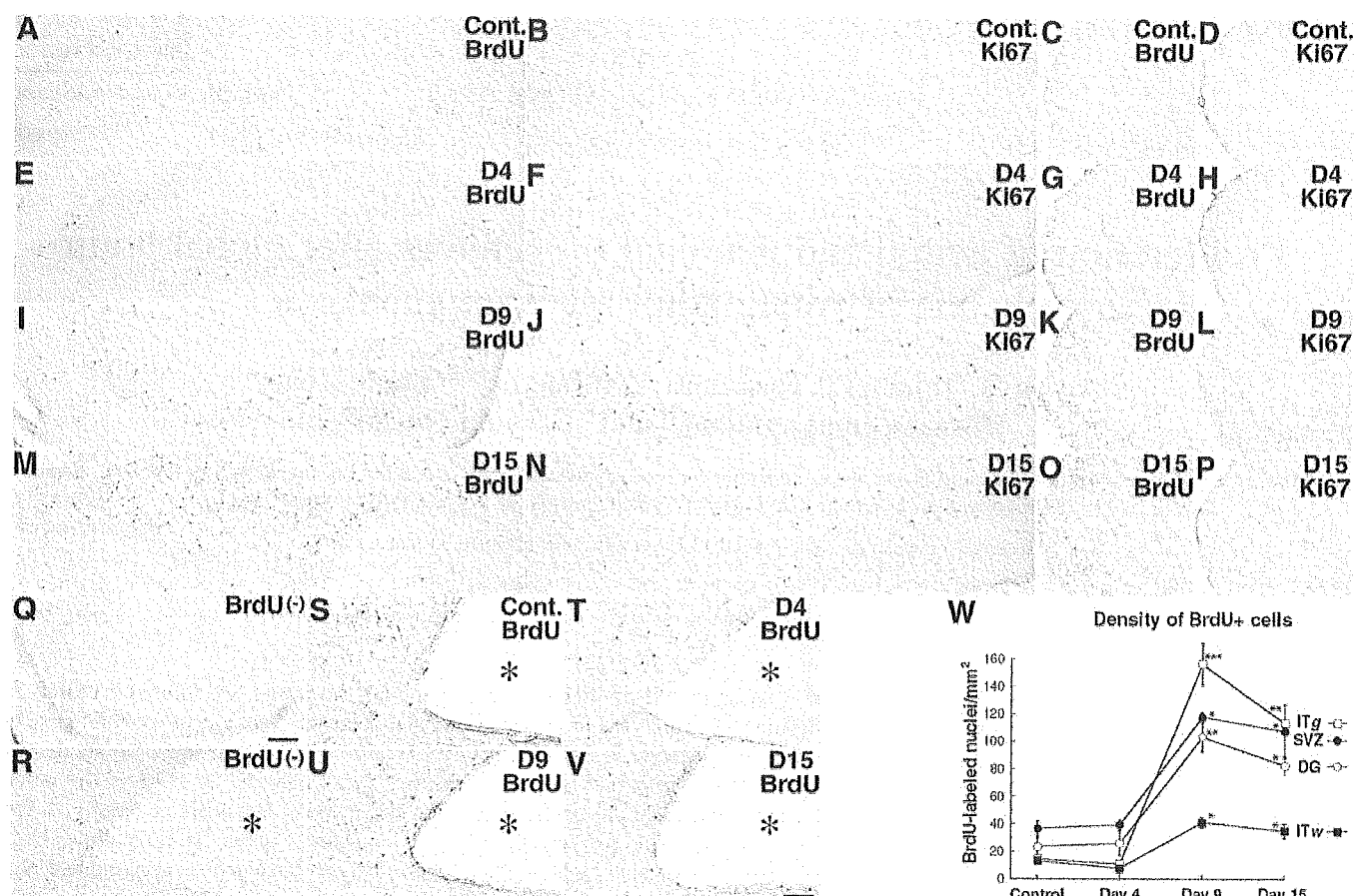


Fig. 1. BrdU and Ki67 immunoreactivity in the macaque DG (A, B, E, F, I, J, M, and N), IT gray matter (C, D, G, H, K, L, O, and P), and SVZ (S–V). Note the greater number of immunopositive nuclei in the posts ischemic Day 9 (D9) and Day 15 (D15) monkey brains compared to the control (Cont.) and posts ischemic Day 4 (D4) ones. Lack of BrdU staining in DG (Q) and SVZ (R) of a monkey not injected with BrdU. Scale bars: A–Q (in Q), 200  $\mu\text{m}$  for DG and 500  $\mu\text{m}$  for IT; R–V (in V), 100  $\mu\text{m}$ . Asterisk, inferior horn of the lateral ventricle. W, density of the BrdU-immunoreactive nuclei in DG, IT gray matter (ITg), SVZ, and IT white matter (ITw). \*\*\*  $P < 0.001$ ; \*\*  $P < 0.01$ ; \*  $P < 0.05$  vs control and Day 4 monkeys.

## Results

### Distribution and number of proliferating cells

Most 5-bromo-2'-deoxyuridine (BrdU)-positive (BrdU+) cells in DG of all monkeys were localized to SGZ (Figs. 1A,E,I, and M). The number of BrdU+ cells increased in the posts ischemic Days 9 and 15 monkey DG, and a similar effect was observed in IT (Figs. 1C,G,K, and O) and SVZ (Figs. 1S–V). The increase was statistically significant (Fig. 1W). We then performed immunolabeling for Ki67, an antigen expressed in all active phases of the cell cycle (Scholzen and Gerdes, 2000). Immunohistochemistry for Ki67 showed a similar distribution and time-dependent increase as BrdU immunoreactivity (Figs. 1B,D,F,H,J,L,N,P). BrdU/Ki67 double staining confirmed the colocalization of the two markers (Figs. 2A–G). The BrdU+/Ki67+ cells were on average 80% of all BrdU+ cells (Table 1); BrdU–/Ki67+ cells were almost never seen.

### Neuronal loss and DNA damage after ischemia

We labeled neurons with an antibody against NeuN, a neuron-selective antigen in the mammalian brain (Mullen et al., 1992). NeuN immunohistochemistry revealed a marked neuronal loss in the posts ischemic CA1 sector (Figs. 2H–K). The average density of NeuN+ cells in the control CA1 was  $567 \pm 26$  cells/ $\text{mm}^2$  vs  $218 \pm 27$  cells/ $\text{mm}^2$  in the posts ischemic CA1 (two-sided  $t$  test,  $P < 0.001$ ). DG and IT displayed a lack of neuronal loss (data not shown). Terminal deoxynucleotidyltransferase-mediated UTP nick end labeling (TUNEL) staining indicative of DNA strand breaks labeled a maximal number of cells in the posts ischemic Day 4 CA1 (Figs. 2L–O), with a few positive cells remaining at Days 9 and 15. TUNEL/NeuN double labeling showed that the TUNEL reaction was selectively localized in the CA1 neurons, and triple labeling with BrdU demonstrated that TUNEL and BrdU stain different cells (Fig. 2Q). In SGZ and SVZ, TUNEL+ cells were rare (on average 1 per